AD-A107 703 ARNOLD ENGINEERING DEVELOPMENT CENTER ARNOLD AFS TN F/G 20/4
NASA/ROCKWELL INTERNATIONAL SPACE SHUTTLE ORBITER YAW HEATING T--ETC(U)
JAN 81 K W NUTT, L A TICATCH

UNCLASSIFIED AEDC-TSR-81-V6 NL

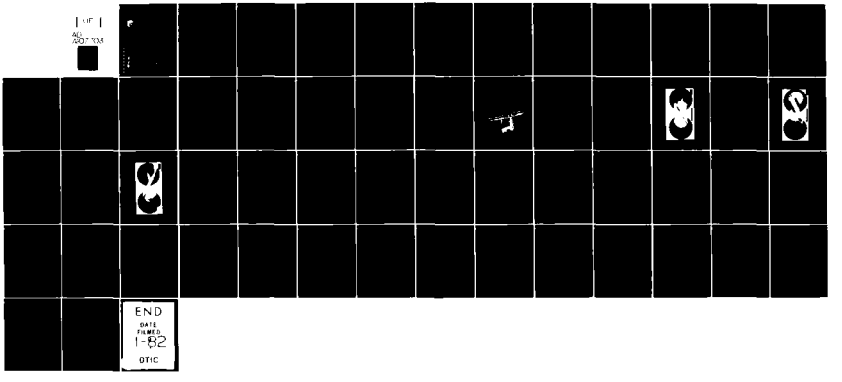

END
DATE FILMED
1-82
DTIC

AEDC-TSR-81-V6

LEVEL 2

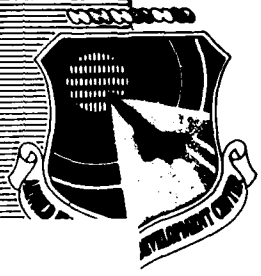

NASA/ROCKWELL INTERNATIONAL SPACE SHUTTLE ORBITER YAW HEATING TEST (OH-109)

K. W. Nutt and L. A. Ticatch
Calspan Field Services, Inc.

January 1981
Final Report for Period 26 October - 24 November 1980

Approved for public release; distribution unlimited.

ARNOLD ENGINEERING DEVELOPMENT CENTER
ARNOLD AIR FORCE STATION, TENNESSEE
AIR FORCE SYSTEMS COMMAND
UNITED STATES AIR FORCE

NOTICES

When U. S. Government drawings, specifications, or other data are used for any purpose other than a definitely related Government procurement operation, the Government thereby incurs no responsibility nor any obligation whatsoever, and the fact that the Government may have formulated, furnished, or in any way supplied the said drawings, specifications, or other data, is not to be regarded by implication or otherwise, or in any manner licensing the holder or any other person or corporation, or conveying any rights or permission to manufacture, use, or sell any patented invention that may in any way be related thereto.

References to named commerical products in this report are not to be considered in any sense as an indorsement of the product by the United States Air Force or the Government.

APPROVAL STATEMENT

This report has been reviewed and approved.

J. T. BEST
Aeronautical Systems Division
Deputy for Operations

Approved for publication:

FOR THE COMMANDER

JOHN M. RAMPY, Assistant Deputy
Aerospace Flight Dynamics Testing
Deputy for Operations

REPORT DOCUMENTATION PAGE		READ INSTRUCTIONS BEFORE COMPLETING FORM
1. REPORT NUMBER AEDC-TSR-81-V 6	2. GOVT ACCESSION NO. AD-A100 703	3. RECIPIENT'S CATALOG NUMBER
4. TITLE (and Subtitle) NASA/ROCKWELL INTERNATIONAL SPACE SHUTTLE ORBITER YAW HEATING TEST (OH-109)		5. TYPE OF REPORT & PERIOD COVERED Final Report - October 26, 1980 - November 24, 1980 6. PERFORMING ORG. REPORT NUMBER
7. AUTHOR(s) K. W. Nutt and L. A. Ticatch, Calspan Field Services, Inc., AEDC Division		8. CONTRACT OR GRANT NUMBER(s)
9. PERFORMING ORGANIZATION NAME AND ADDRESS Arnold Engineering Development Center Air Force Systems Command Arnold Air Force Station, Tennessee 37389		10. PROGRAM ELEMENT, PROJECT, TASK AREA & WORK UNIT NUMBERS Program Element 921E01 Control No. 9E01-00-0
11. CONTROLLING OFFICE NAME AND ADDRESS NASA/Johnson Space Center ES3 Houston, Texas 77058		12. REPORT DATE January 1981 13. NUMBER OF PAGES 52
14. MONITORING AGENCY NAME & ADDRESS(if different from Controlling Office)		15. SECURITY CLASS. (of this report) Unclassified 15a. DECLASSIFICATION/DOWNGRADING SCHEDULE

16. DISTRIBUTION STATEMENT (of this Report)

Approved for public release; distribution unlimited.

17. DISTRIBUTION STATEMENT (of the abstract entered in Block 20, if different from Report)

18. SUPPLEMENTARY NOTES

Available in Defense Technical Information Center (DTIC).

19. KEY WORDS (Continue on reverse side if necessary and identify by block number)

heat transfer
thin skin
phase change paint
space shuttle orbiter
hypersonic testing

20. ABSTRACT (Continue on reverse side if necessary and identify by block number)

Thin-skin thermocouple heat transfer tests were conducted on two 0.0175 scale and one 0.04 scale model of the space shuttle orbiter. In addition, a phase-change paint heat transfer test was conducted on a 0.0175 scale SILTS Pod tail of the orbiter. Oil flow data were also obtained on the orbiter's upper surface. The primary objective of the thin skin thermocouple entry was to obtain better identification of regions of peak heating on the upper surface of the orbiter with attention to the Orbiter Maneuvering System (OMS) pods. The objective of the phase-change paint entry was to establish the peak heating location on the

DD FORM 1 JAN 73 1473 EDITION OF 1 NOV 65 IS OBSOLETE

20. ABSTRACT - continued

orbiter SILTS tail configuration. Data were recorded at Mach 8 in the AEDC-VKF Hypersonic Wind Tunnel B at free stream Reynolds numbers ranging from 0.5 x 10^6 to 3.2 x 10^6. The model angle of attack ranged from 20 to 40 degrees with yaw angle varying from -2 to 2 degrees.

CONTENTS

APPENDIXES

I. ILLUSTRATIONS

Figure

II. TABLES

Table

NOMENCLATURE

ALPI	Indicated pitch angle, deg
ALPHA	Angle of attack, deg
ALPPB	Prebend angle, deg
b	Model skin thickness, in. or ft as noted
B	Wing span, in. (see Fig. 3)
BV	Height of model vertical tail, in. (see Fig. 3)
BETA(TT)	Semi-infinite slab parameter for H based on (TT), [H(TT) • $\sqrt{\text{TIMEEXP}}$]/(PCK)1/2
BETA(0.9TT)	Semi-infinite slab parameter for H based on 0.9TT, [H(0.9TT) • $\sqrt{\text{TIMEEXP}}$],(PCK)1/2
BETA(0.85TT)	Semi-infinite slab parameter for H based on 0.85TT, [H(0.85TT) • $\sqrt{\text{TIMEEXP}}$]/(PCK)1/2
c	Model material specific heat, Btu/lbm-°R
C	Local chord of wing or vertical tail, in. (see Fig. 3)
CAMERA	Denotes camera loations: TOP - top of tunnel, OS - operating side of tunnel (right side looking downstream), NOS - nonoperating side of tunnel (left side looking downstream)
DELTAE	Elevon deflection angle, deg
DELTASB	Speed brake deflection angle, deg
DELTBF	Body flap deflection angle, deg
DTW/DT	Derivative of the model wall temperature with respect to time, °R/sec
H(REF)	Reference heat transfer coefficient (see Appendix III)
H(TR)	Heat transfer coefficient based on TR, QDOT/(TR-TW), Btu/ft^2-sec-°R
H(TT)	Heat transfer coefficient based on TT, QDOT/(TT-TW), Btu/ft^2-sec-°R
H(TRAX)	Heat transfer coefficient calculated using a finite element computer code (Ref. 4)

H(0.9TT)	Heat transfer coefficient based on (0.9TT), QDOT/(0.9TT-TW), Btu/ft^2-sec-°R
H(0.85TT)	Heat transfer coefficient based on (0.85TT), QDOT/(0.85TT-TW), Btu/ft^2-sec-°R
L	Reference length, in. (see Fig. 3)
M, MACH NO.	Free-stream Mach number
MODEL	Orbiter model installed
MU	Dynamic viscosity based on free-stream temperature, lbf-sec/ft^2
MUTT	Dynamic viscosity based on TT, lbf-sec/ft^2
P	Free-stream static pressure, psia
(PCK)1/2, $\sqrt{PCK}$	Square root of the product of the model density, specific heat, and thermal conductivity; Btu/ft^2-sec$^{1/2}$°R
PT	Tunnel stilling chamber pressure, psia
PT2	Stagnation pressure downstream of a normal shock, psia
PHI	Radial angle location of thermocouple in model coordinates, deg (see Figs. 3 and 8)
PHII	Indicated roll angle, deg
Q	Free-stream dynamic pressure, psia
QDOT	Heat-transfer rate, Btu/ft^2-sec
RE	Free-stream unit Reynolds number, ft^{-1}
RHO	Free-stream density, lbm/ft^3
RN	Reference nose radius, (0.0175 ft or 0.04 ft, determined by model scale)
ROLL NO	Identification number for each roll of film
RUN	Data set identification number
STFR	Stanton number based on reference conditions (see Appendix III)
t	Time from start of model injection cycle, sec
t_1	Time when initial model wall temperature was recorded before model injection, sec

T	Free-stream static temperature, °R or °F
TBAR(TT)	(TPC-TI)/(TT-TI)
TBAR(0.9TT)	(TPC-TI)/(0.9TT-TI)
TBAR(0.85T1)	(TPC-TI)/(0.85TT-TI)
TC NO, TC	Thermocouple identification number
TI	Initial wall temperature before injection into the flow, °R or °F
TIME	Elapsed time from lift-off, sec
TIMEEXP	Time of exposure to the tunnel flow when the data were recorded, [TIME - (0.56)(TIMEINJ)], sec
TIMEINJ	Elapsed time from lift-off to arrival at tunnel centerline, sec
TPC	Phase-change paint temperature, °R or °F
TR	Assumed recovery temperature, °R, or °F
TT	Tunnel stilling chamber temperature, °R or °F
TW	Model surface temperature, °R or °F
V	Free-stream velocity, ft/sec
X	Model scale axial coordinate from model nose or leading edge of wing or vertical tail (see Figs. 3 and 8), in.
XO	Full scale axial coordinate from a point 235 in. ahead of the orbiter nose (see Fig. 8), in.
X/L	Thermocouple axial location as a ratio of model length from model nose tip
Y	Model scale lateral coordinate (see Fig. 3), in.
YAW	Yaw angle of model, deg
YO	Full scale lateral coordinate, in.
Z	Model scale vertical coordinate (see Fig. 3), in.
ZO	Full scale vertical coordinate, in.
β	Semi-infinite slab parameter, H(TR) $\sqrt{\text{TIMEEXP}}/\sqrt{\text{PCK}}$
ρ	Model material density, lbm/ft^3

1.0 INTRODUCTION

The work reported herein was conducted by the Arnold Engineering Development Center (AEDC), Air Force Systems Command (AFSC), under Program Element 921E01, Control Number 9E01-00-0, at the request of the Johnson Space Center (NASA-JSC(ES3)), Houston, Texas. The NASA-JSC (ES3) program manager was Mrs. Dorothy B. Lee and the Rockwell International project engineer was Mr. Jim Collins. The results were obtained by Calspan Field Services, Inc./AEDC Division, operating contractor for the Aerospace Flight Dynamics testing effort at the AEDC, AFSC, Arnold Air Force Station, Tennessee. The tests were conducted in the von Karman Gas Dynamics Facility (VKF), under AEDC Project No. C062VB.

The test was conducted in the 50-in.-diam Hypersonic Wind Tunnel (B) at the von Karman Gas Dynamics Facility (VKF) during the period October 26, 1980 to November 24, 1980. Data were recorded at Mach number 8 for nominal Reynolds numbers ranging from 0.5×10^6 to 3.7×10^6 per foot. The nominal model angles of attack ranged from 20 to 40 degrees with model yaw angles varying from -2 to 2 degrees. All thin-skin thermocouple data were obtained from three space shuttle orbiter models designated (1) 56-0 (0.0175 scale), (2) 60-0 (0.0175 scale), and (3) 83-0 (0.04 scale). The phase-change paint model was also a 0.0175 scale model of the 56-0 series.

This test had a NASA/Rockwell designation of OH-109. The objective of the thin-skin thermocouple phase of the test was to obtain additional heating data for identification of regions of peak heating on the orbiter in yaw. The objective of the phase-change paint entry was to establish the peak heating location for the SILTS* pod located on the orbiter vertical tail.

Copies of all the detailed test logs have been transmitted to Rockwell International. Three copies of the final tabulated data are being transmitted with this report to Rockwell International. Data tapes have been transmitted to Chrysler Corporation Space Division for their use under the Dataman contract. Inquiries to obtain copies of the test data should be directed to NASA-JSC(ES3), Houston, Texas 77058. A microfilm record has been retained in the VKF at AEDC.

2.0 APPARATUS

2.1 TEST FACILITY

Tunnel B (Fig. 1, Appendix I) is a closed circuit hypersonic wind tunnel with a 50-in. diam test section. Two axisymmetric contoured nozzles are available to provide Mach numbers of 6 and 8, and the tunnel

*Shuttle Infrared Leeside Temperature Sensor (SILTS)

may be operated continuously over a range of pressure levels from 20 to 300 psia at Mach number 6, and 50 to 900 psia at Mach number 8, with air supplied by the VKF main compressor plant. Stagnation temperatures sufficient to avoid air liquefaction in the test section (up to 1350°R) are obtained through the use of a natural gas fired combustion heater. The entire tunnel (throat, nozzle, test section, and diffuser) is cooled by integral, external water jackets. The tunnel is equipped with a model injection system, which allows removal of the model from the test section while the tunnel remains in operation. A description of the tunnel may be found in Ref. 1.

2.2 TEST ARTICLES

Three space shuttle orbiter models were used to obtain the thin-skin thermocouple data for this test. Two of the test articles were 0.0175 scale models of the full orbiter and were designated as the 60-0 and 56-0 models. The third model was a 0.04 scale of the front half of the orbiter and was identified as the 83-0 model. All of the models were supplied by Rockwell International.

The 60-0 model was a 0.0175 scale thin-skin thermocouple model of the Rockwell International Vehicle 5 configuration. The model was constructed of 17-4 PH stainless steel with a nominal skin thickness of 0.030 in. at the instrumented areas. All thermocouples were spot welded to the thin-skin inner surface.

A sketch of the 60-0 model installation in the tunnel is shown in Fig. 2. The basic dimensions and coordinate definitions for the 0.0175 scale models are shown in the sketch presented in Fig. 3. The deflection angles of the speedbrake and elevons were varied during this test and recorded on the tabulated data. The body flap was set at a zero deflection angle throughout the test.

The 56-0 model used for the thin-skin thermocouple portion of the test was model number 2B of the material "LH" 56-0 phase change paint model series. This was a 0.0175 scale model with the same external contour as the 60-0 model. The pilot side (left) of the fuselage has been replaced with a thin-skin thermocouple insert contoured to the vehicle lines. This insert was constructed of 17-4 PH stainless steel with a nominal skin thickness of 0.020 in. at the thermocouple locations. A photograph of the 56-0 model injected in the tunnel is shown in Fig. 4. A sketch of the 56-0 model installation is shown in Fig. 5. The dimensions and coordinate system presented in Fig. 3 also apply to the 0.0175 scale 56-0 model.

The 83-0 model was a 0.04 scale model of the forward half of the orbiter. This model was also constructed of 17-4 PH stainless steel with a nominal skin thickness of 0.030 in. A photograph of the 83-0 model injected in the tunnel is shown in Fig. 6. The installation sketch of the 83-0 model is shown in Fig. 7, and the coordinate system and basic dimensions for the 83-0 model are presented in Fig. 8.

The model used for the phase change paint entry was from the 56-0 series constructed without the thin-skin thermocouple insert. Two 0.0175 scale removable vertical tails with the SILTS pod were fabricated of Novamide 700-55. A photograph of this model injected in the tunnel is shown in Fig. 9.

2.3 TEST INSTRUMENTATION

2.3.1 Test Conditions

The instrumentation, recording devices, and calibration methods used to measure the primary tunnel and test data parameters are listed in Table 1a along with the estimated measurement uncertainties. The range and estimated uncertainties for primary parameters that were calculated from the measured parameters are listed in Table 1b.

2.3.2 Test Data

The 60-0 model was instrumented with 600 thirty-gauge iron-constanton and chromel-constantan thermocouples. Only 230 of these thermocouples were used on this test. Thermocouple locations for this model are illustrated in Fig. 10; the dimensional locations and skin thickness for the thermocouples connected on this test are listed in Table 2. The thermocouples identified by a number only are iron-constantan. The thermocouples identified by a number followed by the letter A or C are Chromel®-constantan that were added to the model. The letter D after a thermocouple number designates an iron-constantan thermocouple in a new location on the OMS pod.

The 56-0 model instrumentation consisted of 80 thirty-gauge Chromel-constantan thermocouples located on the thin-skin insert. All of these thermocouples were connected on this test. The thermocouple locations for this model are illustrated in Fig. 11. The dimensional locations and skin thicknesses are listed in Table 3.

For this test only 94 of the 482 thirty-gauge Chromel-constantan thermocouples on the 83-0 model were connected. The thermocouple locations for this model are illustrated in Fig. 12. The dimensional locations and skin thicknesses for the thermocouples used on this test are included in Table 4.

The thermocouple data were recorded on a new* multiplexing system that is capable of recording a maximum of 256 thermocouple channels during each run. This increased capacity greatly increases efficiency by reducing the need for multiple runs. The maximum number of thermocouples recorded during one run was 230 when the 60-0 model was installed. All 80 thermocouples were connected on the 56-0 model, and 94 were connected on the 83-0 model. Some of the listed thermocouples were determined to be inoperative during the test, and these have been deleted from the tabulated data.

*The old system was limited to 100 channels per run.

The phase-change paint technique of obtaining heat-transfer data uses a fusible coating which changes from an opaque solid to a transparent liquid (i.e., it melts) at a specified temperature (TPC). The demarcations between melted and unmelted paint (melt lines) are model surface isotherms and are used to compute the aerodynamic heating. Tempilaq paint was used as the phase-change coating for these tests. The calibrated melting points of the paints used were 250, 300, 350, 450, 550, 600 and 700°F. A more complete description of the phase-change paint technique is presented in Ref. 2.

3.0 TEST DESCRIPTION

3.1 TEST CONDITIONS

The test was conducted at a nominal Mach number of 8 in Tunnel B. A summary of the specific test conditions is given below.

MACH NO.	PT, psia	TT, °R	Q, psia	P, psia	RE x 10^{-6}, ft^{-1}
7.83	100	1250	0.5	0.010	0.5
7.84	120	1245	0.6	0.014	0.6
7.88	205	1260	1.0	0.020	1.0
7.93	435	1300	2.0	0.050	2.0
7.96	670	1320	3.1	0.070	3.0
7.97	850	1350	3.9	0.090	3.7

A more detailed test summary showing all configurations tested and the variables for each is presented in Table 5.

3.2 TEST PROCEDURE

3.2.1 General

In the VKF continuous flow wind tunnels (A, B, C), the model is mounted on a sting support mechanism in an installation tank directly underneath the tunnel test section. The tank is separated from the tunnel by a pair of fairing doors and a safety door. When closed, the fairing doors, except for a slot for the pitch sector, cover the opening to the tank, and the safety door seals the tunnel from the tank area. After the model is prepared for a data run, the personnel access door to the installation tank is closed, the tank is vented to the tunnel flow, the safety and fairing doors are opened, and the model is injected into the airstream. After the data are obtained, the model is retracted into the tank and the sequence is reversed with the tank being vented to atmosphere to allow access to the model in preparation for the next run. A given injection cycle is termed a run, and all the data obtained are identified in the data tabulations by a run number.

3.2.2 Thin-Skin Thermocouple

Prior to each test run, the model temperatures were monitored to ensure that they were nominally 70°F. The model was then injected at the desired test attitude as the data acquisition sequence commenced.

The model remained on the tunnel centerline for about three seconds and was then retracted into the installation tank. The model was then cooled and repositioned for the next injection.

A 256 channel multiplexing analog-to-digital converter was used in conjunction with a Digital Equipment Corporation (DEC) PDP-11 computer and a DEC-10 computer to record the temperature data. The system sampled the output of each thermocouple approximately 17 times per second.

3.2.3 Phase-Change Paint

For phase-change paint tests the model was painted with the appropriate Tempilaq paint, and the model surface initial temperature (TI) was measured with a thermocouple probe. The model was positioned to the test attitude and injected into the tunnel flow for about 10 sec. During this time three 70-mm sequence cameras using color film photographed the progression of the paint melt lines. These cameras were triggered simultaneously at a nominal rate of two frames/sec while an analog-to-digital scanner recorded the precise timing. After the model was retracted from the tunnel flow, it was cooled and cleaned with an alcohol bath before being repainted for the next test run. For this test only the vertical tail and the SILTS pod were painted with phase-change paint.

Instrumentation outputs were recorded using the VKF data acquisition system under the control of a PDP 11/40 computer. The triggering of the cameras and the frame rate were controlled by a separate control system.

3.2.4 Oil-Flow

Preparation of the model for an oil-flow run was the same as for the phase-change paint runs except that oil was applied to the model in place of the paint. Four sequence cameras were used to photograph the oil-flow patterns.

3.3 DATA REDUCTION

3.3.1 Thin-Skin Thermocouple Data

The reduction of thin-skin temperature data to coefficient form normally involves only the calorimeter heat balance for the thin skin as follows:

$$QDOT = \rho bc\ DTW/DT \tag{1}$$

$$H(TR) = \frac{QDOT}{TR-TW} = \frac{\rho bc\ DTW/DT}{TR-TW} \tag{2}$$

Thermal radiation and heat conduction effects on the thin-skin element are neglected in the above relationship and the skin temperature

response is assumed to be due to convective heating only. It can be shown that for constant TR, the following relationship is true:

$$\frac{d}{dt}\left(\ln\left[\frac{TR-TI}{TR-TW}\right]\right) = \frac{DTW/DT}{TR-TW} \tag{3}$$

Substituting Eq. (3) in Eq. (2) and rearranging terms yields:

$$\frac{H(TR)}{\rho bc} = \frac{d}{dt}\left(\ln\left[\frac{TR-TI}{TR-TW}\right]\right) \tag{4}$$

By assuming that the value of $H(TR)/\rho bc$ is a constant it can be seen that the derivative (or slope) must also be constant. Hence, the term

$$\ln\left[\frac{TR-TI}{TR-TW}\right]$$

is linear with time. This linearity assumes the validity of Eq. (2) which applies for convective heating only. The evaluation of conduction effects will be discussed later.

The assumption that H(TR) and c are constant are reasonable for this test although small variations do occur in these parameters. The variations of H(TR) caused by changing wall temperature and by transition movement with wall temperature are trival for the small wall temperature changes that occur during data reduction. The value of the model material specific heat, c, was computed by the relation

$$c = 0.0797 + (5.556 \times 10^{-5})TW, \text{ (17-4 PH stainless steel)} \tag{5}$$

The maximum variation of c over any curve fit was less than 1.5 percent. Thus, the assumption of constant c used to derive Equation 4 was reasonable. The value of density used for the 17-4 PH stainless steel skin was $\rho = 490$ lbm/ft^3, and the skin thickness, b, for each thermocouple is listed in Tables 2, 3 or 4.

The right side of Equation 4 was evaluated using a linear least squares curve fit of 15 consecutive data points to determine the slope. The start of the curve fit coincided with the model arrival on the tunnel centerline. For each thermocouple the tabulated value of H(TR) was calculated from the slope and the appropriate values of ρbc; i.e.,

$$H(TR) = \rho bc \frac{d}{dt}\left(\ln\left[\frac{TR-TI}{TR-TW}\right]\right) \tag{6}$$

To investigate conduction effects a second value of H(TR) was calculated at a time one second later. A comparison of these two values was used to identify those thermocouples that were influenced by significant conduction (or system noise). The data for a given thermocouple were deleted* if the values of H(TR) differed by more than 35 percent. In general, conduction and/or noise effects were found to be negligible.

*The word DELETE is used on the tabulated data to identify these thermocouples.

Since the value of TR is not known at each thermocouple location, it has become standard procedure to use three assumed values of TR. The assumed values are 1.0TT, 0.9TT and 0.85TT. The use of these assumed values of TR provides an indication of the sensitivity of the heat-transfer coefficients to the value of TR assumed. As can be noted in the tabulated data, there are large percentage differences in the values of the heat-transfer coefficients calculated from the three assumed values. Therefore, if the data are to be used for flight predictions, the value selected for TR is obviously very important and is a function of model location and boundary layer state.

The heat-transfer coefficient calculated from Eq. 4 was normalized using the Fay-Riddell stagnation point coefficient, H(REF), based on a nose radius of 1.0 ft full scale (see Appendix III). The reference nose radius, RN, used to calculate HREF is either 0.0175 ft or 0.04 ft as determined by the model scale.

3.3.2 Phase-Change Paint Data

For phase-change paint tests, the data were reduced by assuming that the model wall heating can be represented by a thermally semi-infinite slab. A material with a low thermal diffusivity is necessary for this assumption to be valid for reasonable model wall thicknesses (>0.25 in.) consistent with the Tunnel B data acquistion times of 3 to 30 sec.

Data reduction of the melt line photographs was accomplished by identifying these isothermal lines for various times during the test run. These isothermal lines are related to corresponding aerodynamic heat-transfer coefficients, H(TR), by applying the semi-infinite slab heat equation, given below.

$$\frac{TPC-TI}{TR-TI} = 1 - e^{\beta^2} \operatorname{erfc} \beta \tag{7}$$

where

$$\beta = \frac{H(TR)\sqrt{TIMEEXP}}{\sqrt{PCK}} \tag{8}$$

and

TIMEEXP = time of heating

The lumped material thermophysical property $\sqrt{PCK}$ for the Novamide 700-55 material was provided by Rockwell. The value of $\sqrt{PCK}$ was a function of temperature, and the values used are listed in Table 6. The heat-transfer coefficients were computed for assumed adiabatic recovery temperatures TT, 0.9TT, and 0.85 TT except when the paint temperature was 700°F. In this case only TT was used because of the small difference between TT and TPC. The Fay-Riddell stagnation point heat-transfer coefficient (Appendix III), based on a 0.0175-ft-radius sphere, was used to normalize the computed aerodynamic heat-transfer coefficients. (The radius of this hypothetical sphere would be 1 ft at corresponding Orbiter full-scale conditions).

The tabulated data is based on the assumption of a semi-infinite slab. In the case of the SILTS pod with a small radius (0.187 in.) the actual heat transfer coefficient values will deviate from those calculated based on the semi-infinite slab assumption. A finite element computer program, Ref. 4, was used to model the SILTS pod geometry and to compute the heat-transfer coefficient at the stagnation point. The heat-transfer coefficient determined from the semi-infinite slab assumption, H(TT), is ratioed to the computed value H(TRAX) for the stagnation point in Fig. 13. The application of this "correction factor" to the data is illustrated in the following example. Consider a case where the tabulated data (based on semi-infinite slab) was obtained at 5 sec and the level of the heat transfer coefficient was 0.02. From Fig. 13 this gives a value of H(TT)/H(TRAX) = 1.3. Thus to adjust (ADJ) the semi-infinite slab tabulated data to that of an axisymmetric element on the hemispherical nose cap we have

$$H(TT)_{ADJ} = \left[H(TT)_{TAB\ DATA}\right]\left[\frac{1}{\frac{H(TT)}{H(TRAX)}}\right] \tag{9}$$

$$= 0.02\left[\frac{1}{1.3}\right]$$

$$= 0.0154 \quad \text{i. e. } \approx 23\% \text{ lower than tabulated data.}$$

It is important to emphasize that the intent of Fig. 13 is only to provide an estimate of the approximate magnitude of the 3-D effects and it is not intended that all the data be "corrected" for 3-D effects.

An accurate estimate of the precision of phase-change paint data is also hampered by the fact that an observer must determine the location of the melt line (Ref. 5). For the results presented in this report only uncertainties attributable to the measured parameters are considered. The nominal uncertainties in these specific parameters are summarized in Table 1b.

3.4 UNCERTAINTY OF MEASUREMENTS

In general, instrumentation calibrations and data uncertainty estimates were made using methods recognized by the National Bureau of Standards (NBS). Measurement uncertainty is a combination of bias and precision errors defined as:

$$U = \pm(B + t_{95}S)$$

where B is the bias limit, S is the sample standard deviation and t_{95} is the 95th percentile point for the two-tailed Student's "t" distribution (95-percent confidence interval), which for sample sizes greater than 30 is taken equal to 2.

Estimates of the measured data uncertainties for this test are given in Table 1a. The data uncertainties for the measurements are

determined from in-place calibrations through the data recording system and data reduction program.

Propagation of the bias and precision errors of measured data through the calculated data was made in accordance with Ref. 3, and the results are given in Table 1b.

4.0 DATA PACKAGE PRESENTATION

Heat-transfer coefficients were obtained at selected locations on the 56-0, 60-0, and 83-0 models of the space shuttle orbiter. Sample tabulated data are presented in Appendix IV. The final tabulated and plotted data were transmitted with this report to NASA-JSC and Rockwell International.

Representative data from the upper centerline (PHI = 180 deg) of the 83-0 model are presented in Fig. 14. Data from two runs are presented as a sample of data repeatability.

REFERENCES

1. Test Facilities Handbook (Eleventh Edition). "von Karman Gas Dynamics Facility, Vol. 3." Arnold Engineering Development Center, June 1979.

2. Jones, Robert A. and Hunt, James L. "Use of Fusible Temperature Indicators for Obtaining Quantitative Aerodynamic Heat-Transfer Data." NASA-TR-R-230, February 1966.

3. Thompson, J. W. and Abernethy, R. B. et al. "Handbook Uncertainty in Gas Turbine Measurements." AEDC-TR-73-5 (AD755356), February 1973.

4. Rochell, J. K. "TRAX- A Finite Element Computer Program for Transient Heat Conduction Analysis of Axisymmetric Bodies." University of Tennessee Space Institute Master's Thesis, June 1973.

5. Nossaman, G. O. "Feasibility Study for Automatic Reduction of Phase Change Imagery." NASA CR-112001, 1971.

APPENDIX I

ILLUSTRATIONS

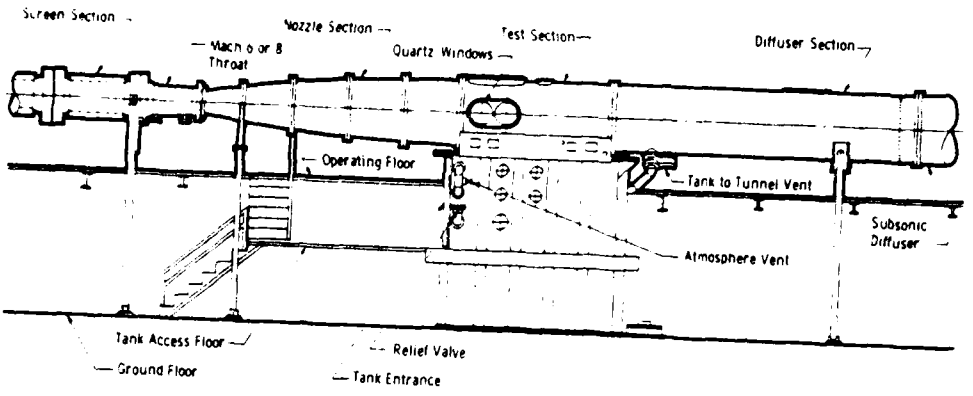

a. Tunnel assembly

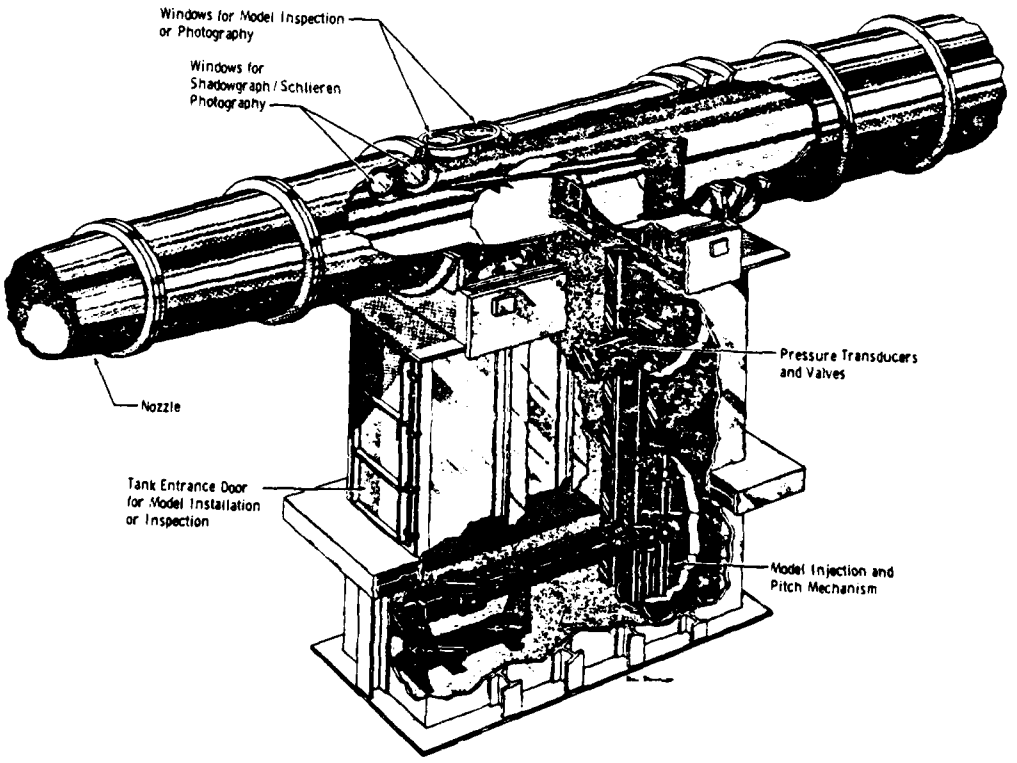

b. Tunnel test section

Fig. 1. Tunnel B

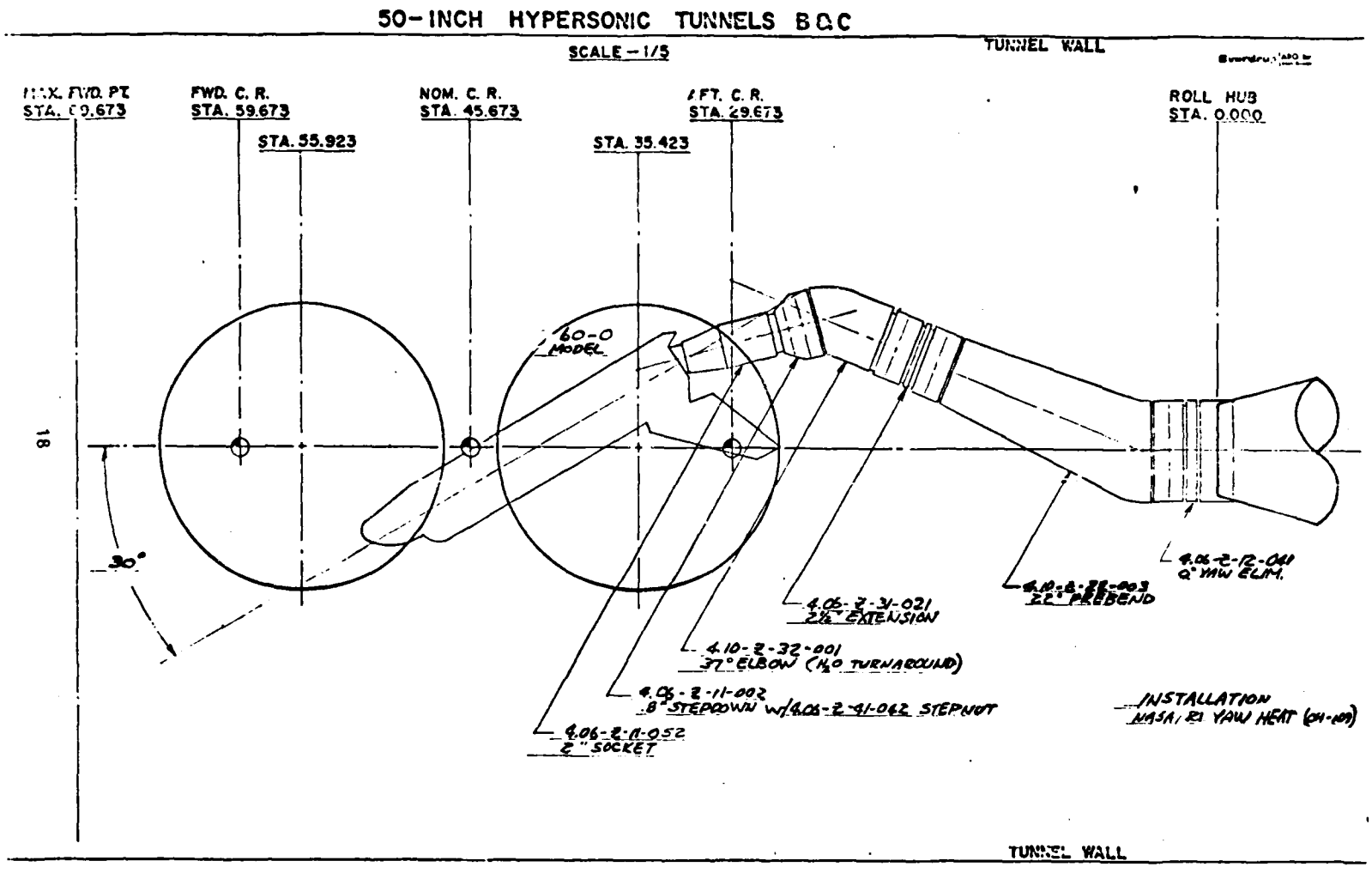

Fig. 2. 60-0 Model Installation

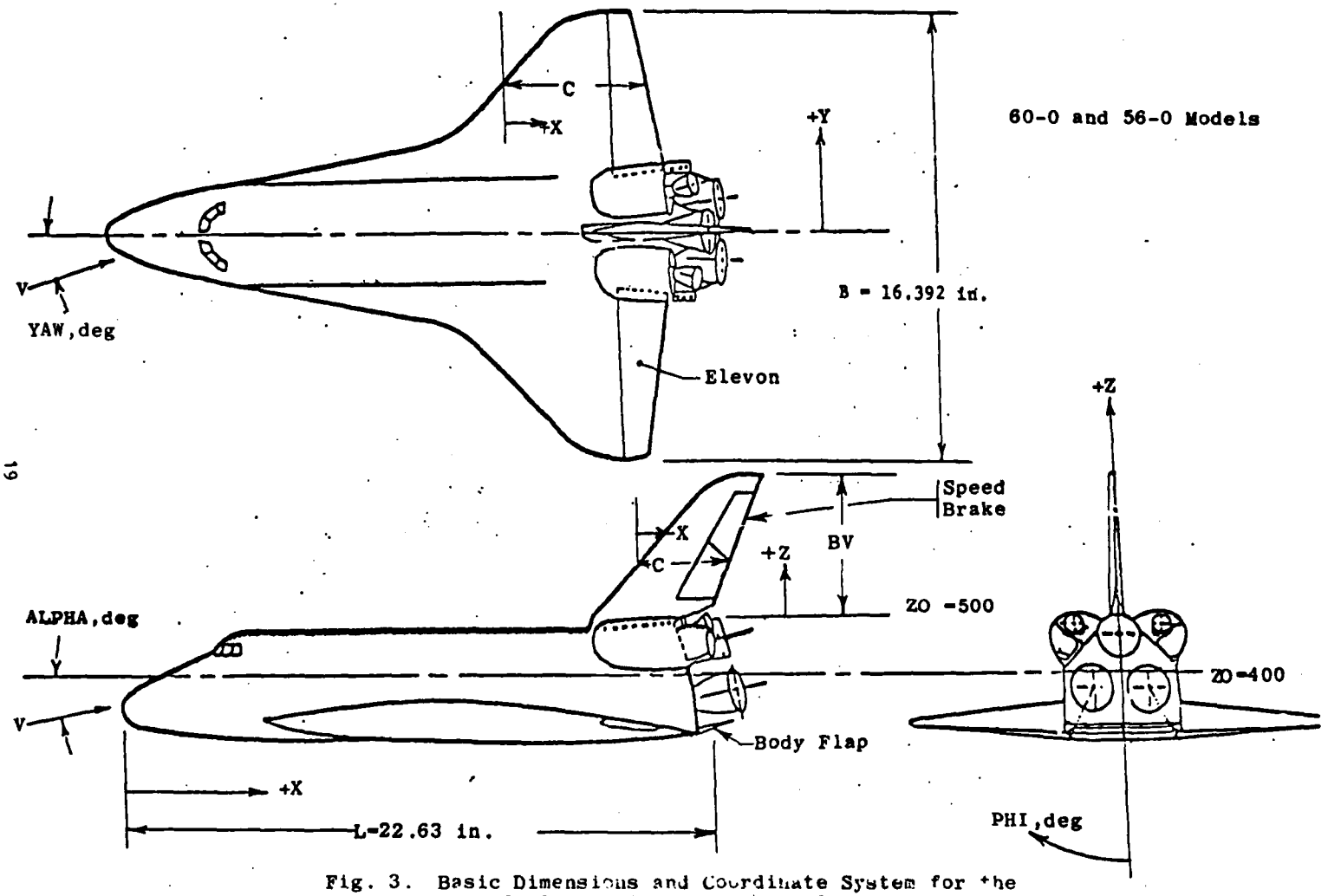

Fig. 3. Basic Dimensions and Coordinate System for the 0.0175 Scale Orbiter Models

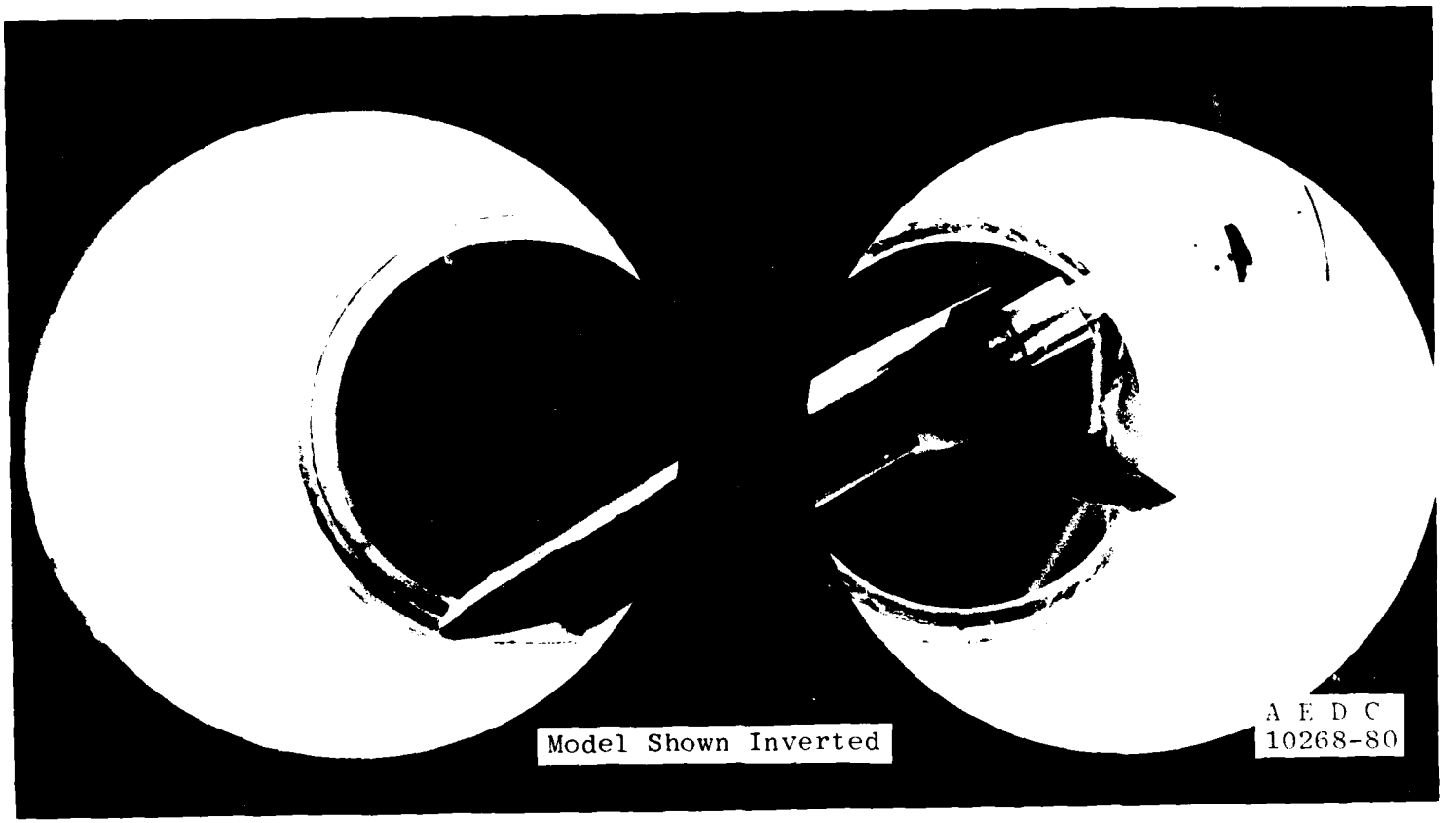

Figure 4. Installation Photograph of 56-0 Model

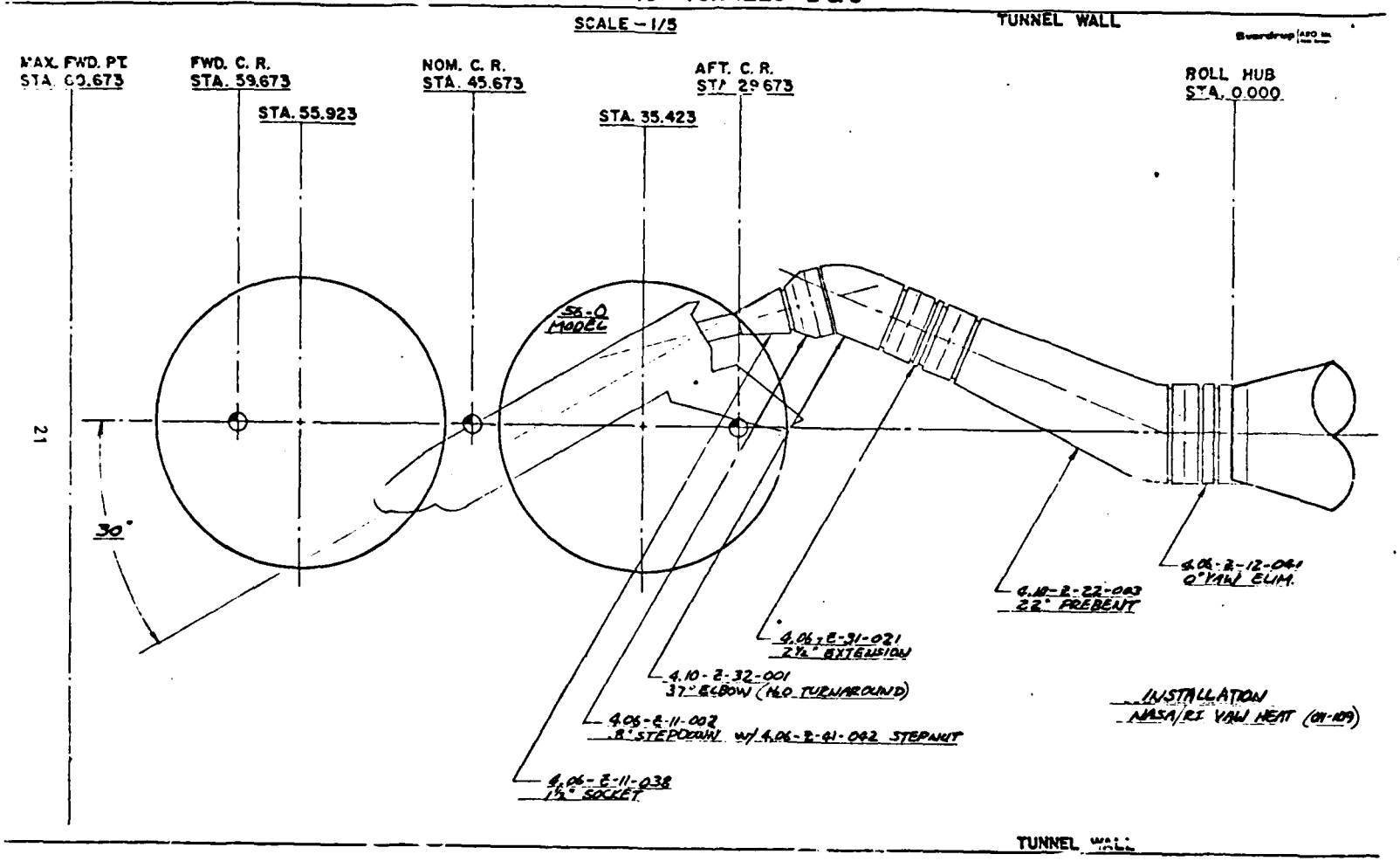

Fig. 5. 56-0 Model Installation for Thin-Skin Thermocouple Test

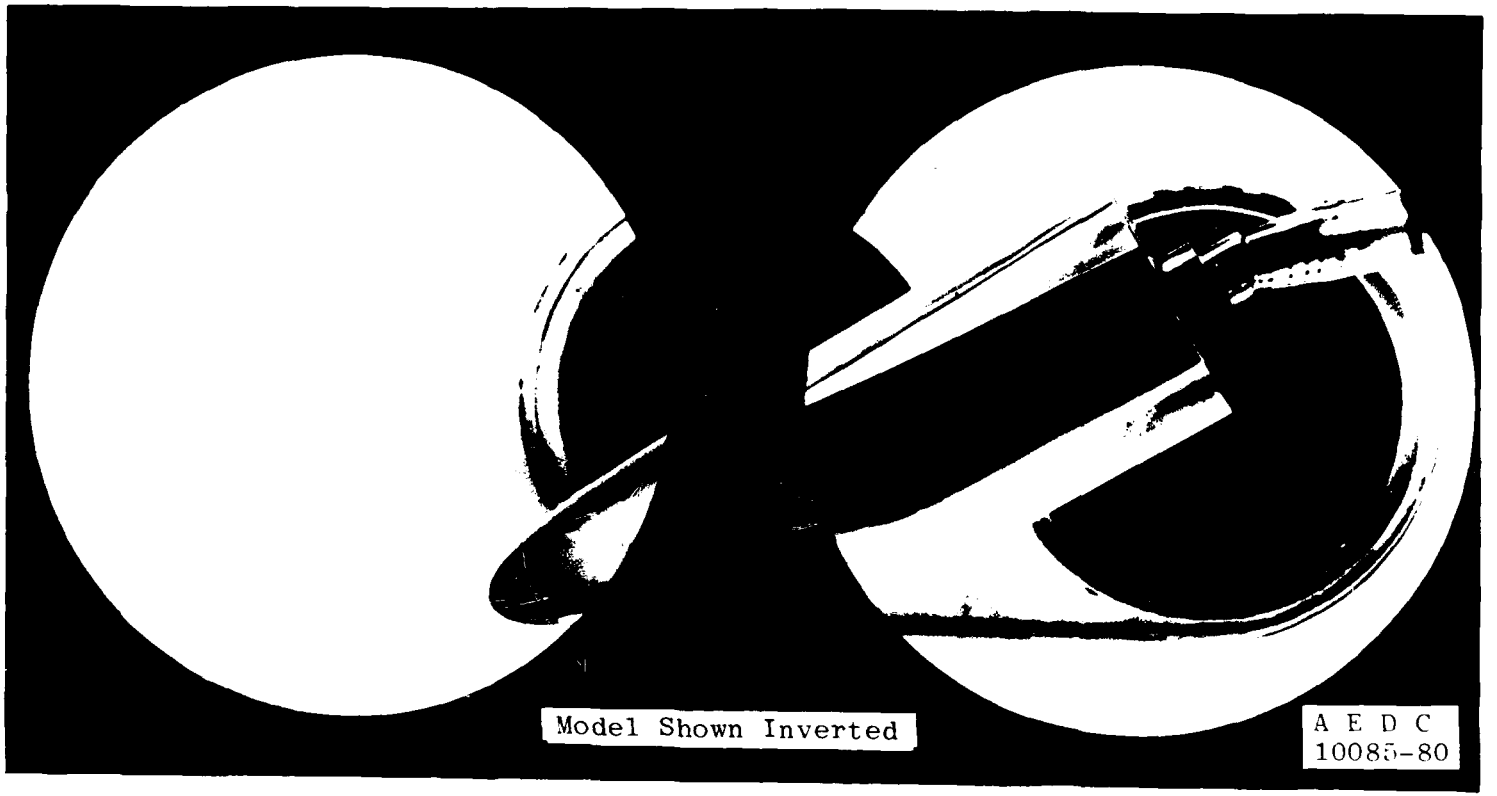

Figure 6. Installation Photograph of 83-0 Model

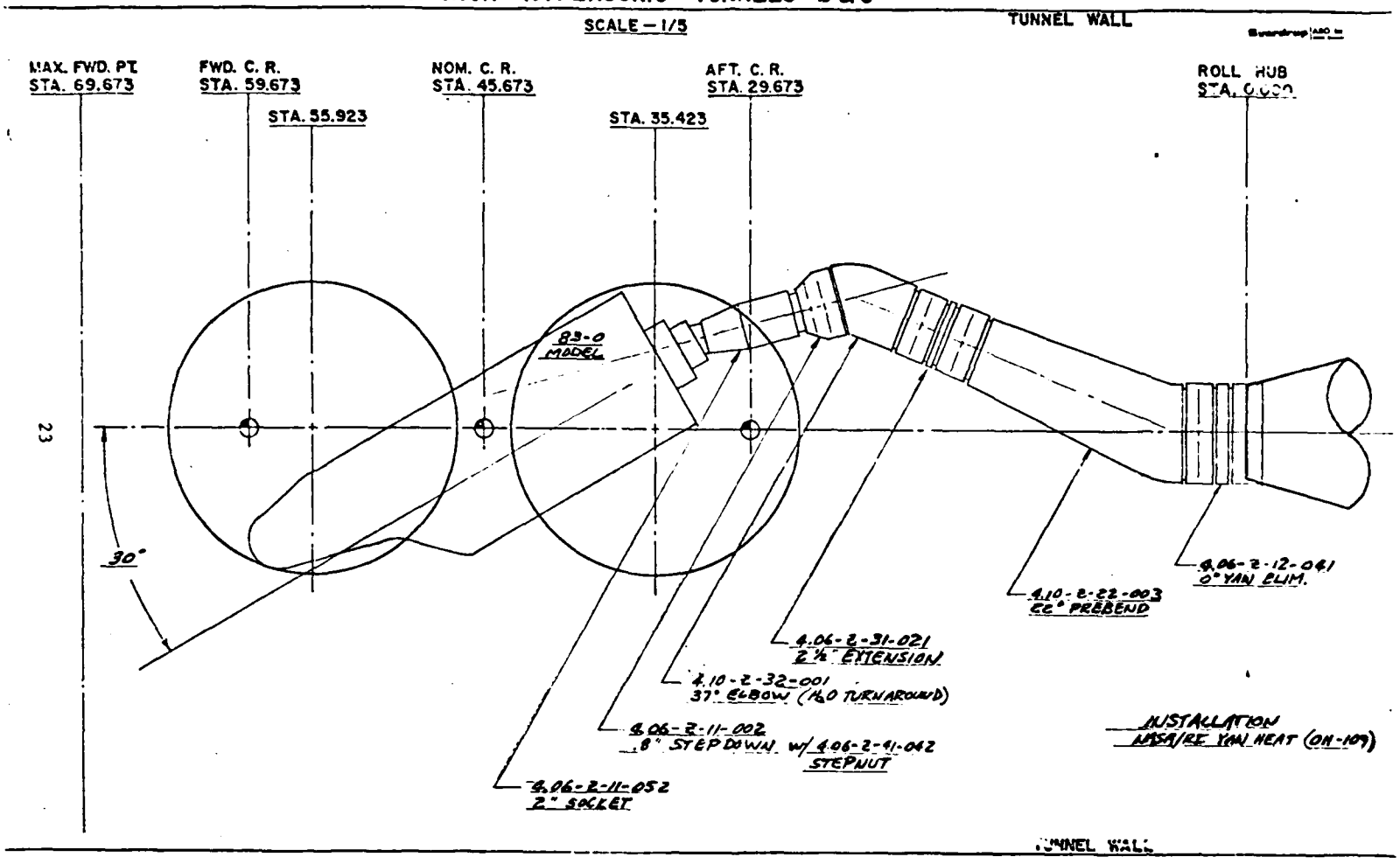

Fig. 7. 83-0 Model Installation

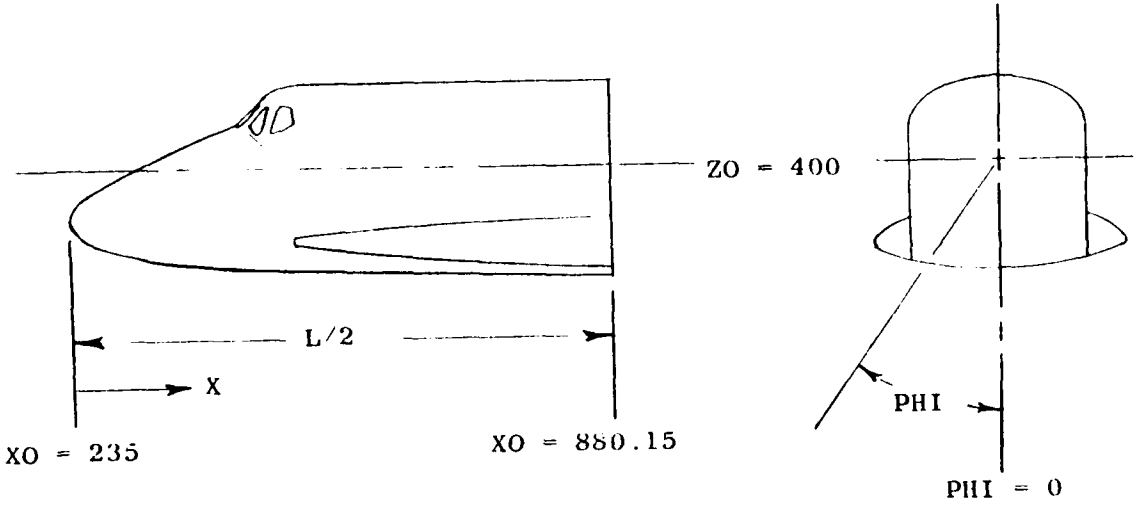

Fig. 8. Basic Dimensions and Coordinate System for the 83-0 Model

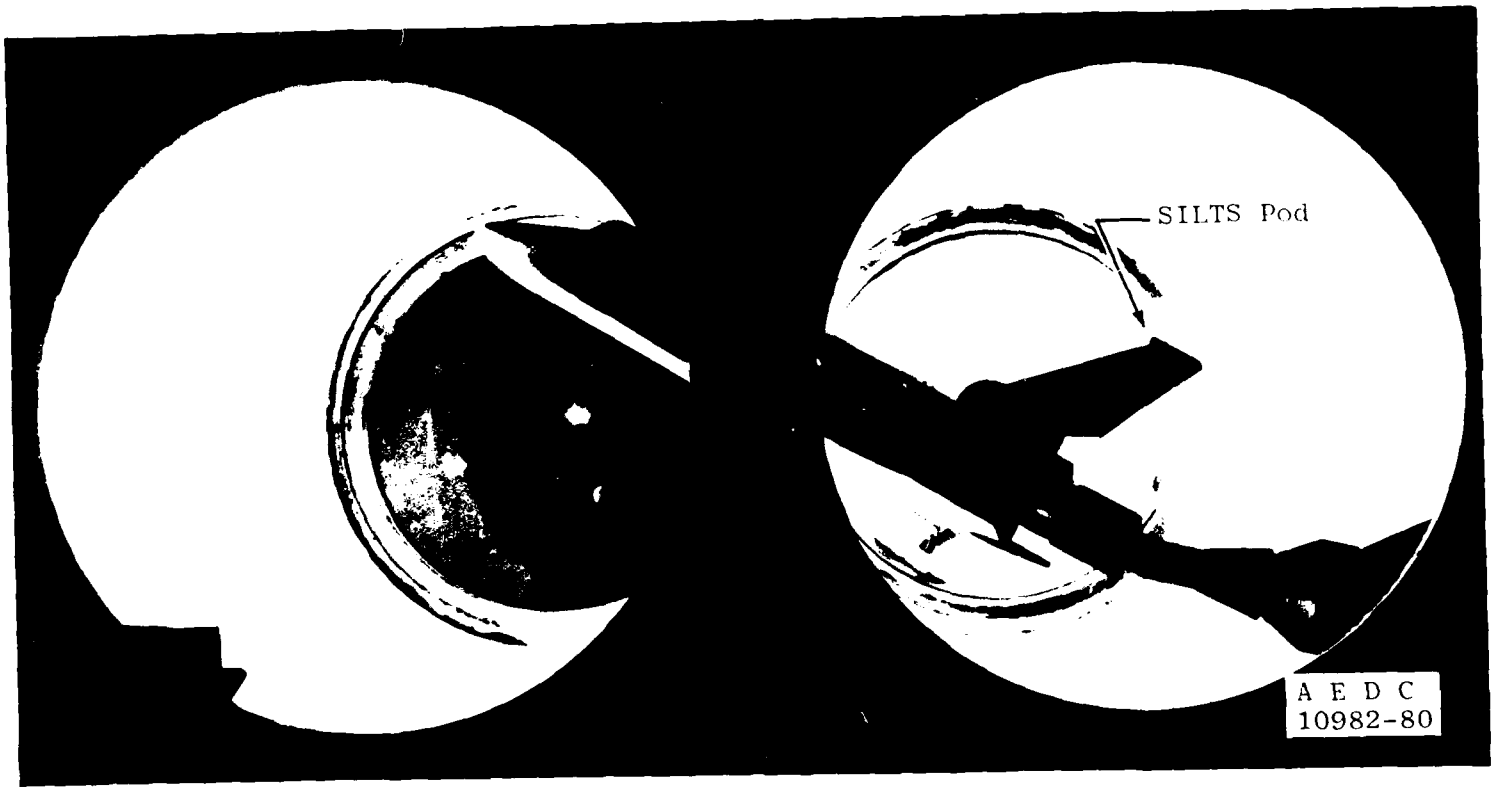

Figure 9. Installation Photograph of Phase Change Paint Model

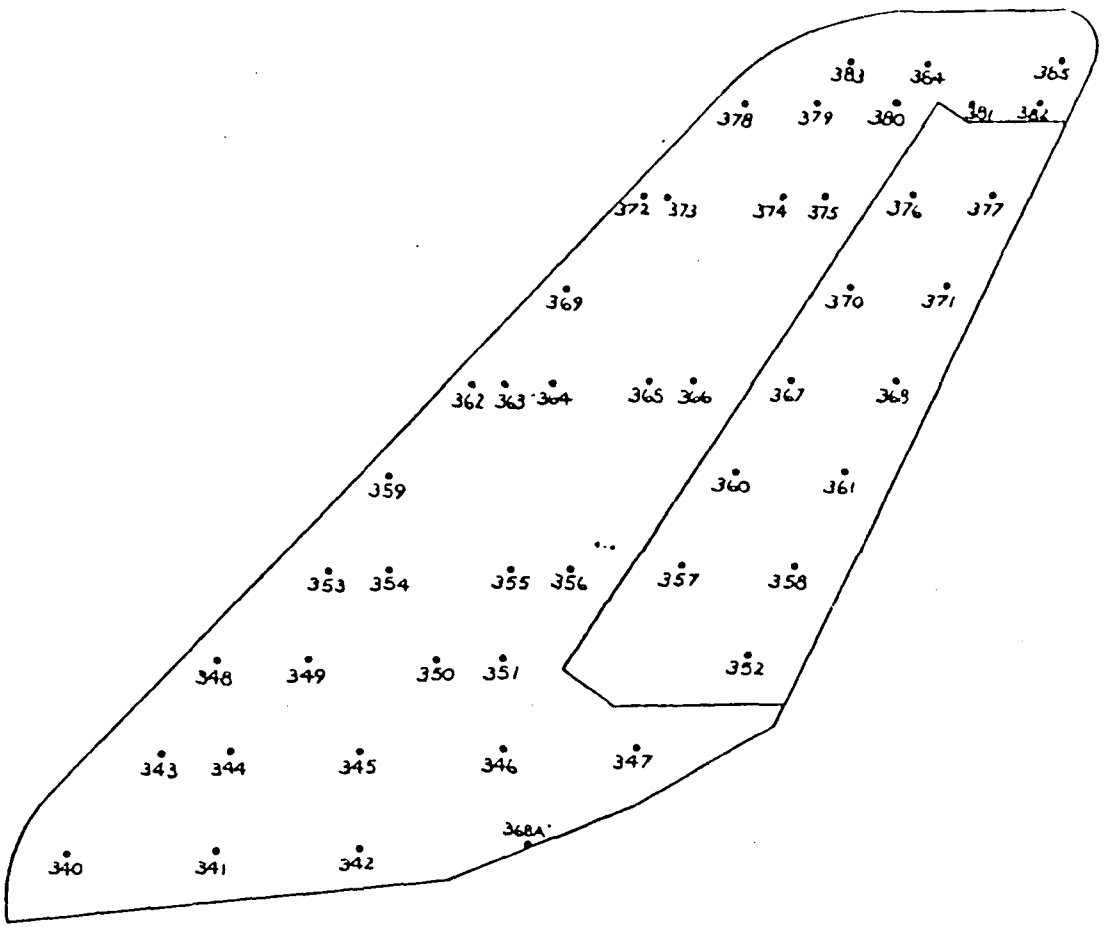

a. Vertical Tail

Fig. 10. Thermocouple Locations on 60-0 Model

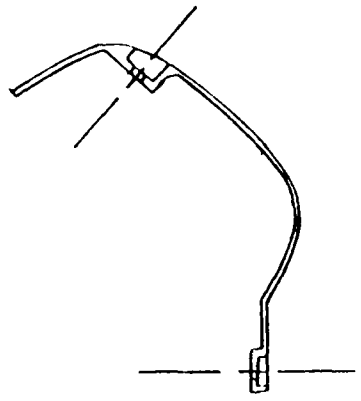

SECTION A-A

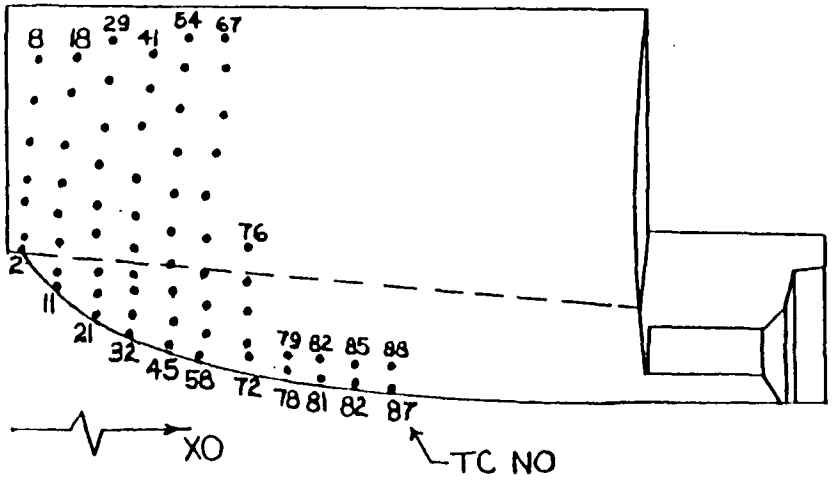

NOTE: FOR CLARITY, NOT ALL TC NO. SHOWN.

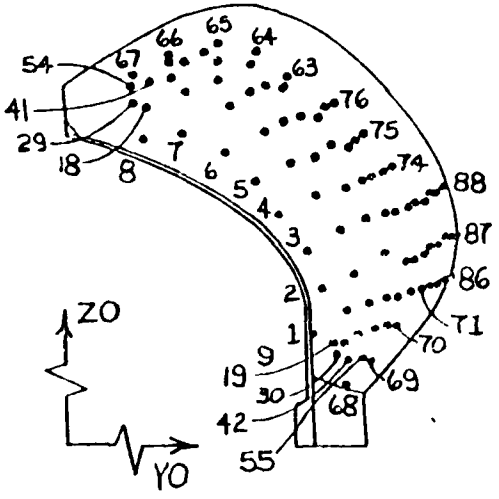

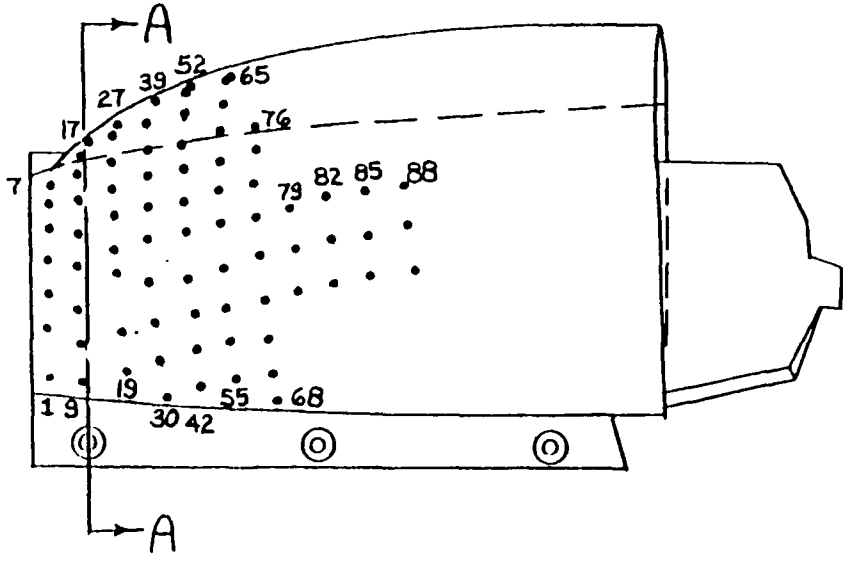

b. OMS Pod Thermocouple Locations
Fig. 10. Continued

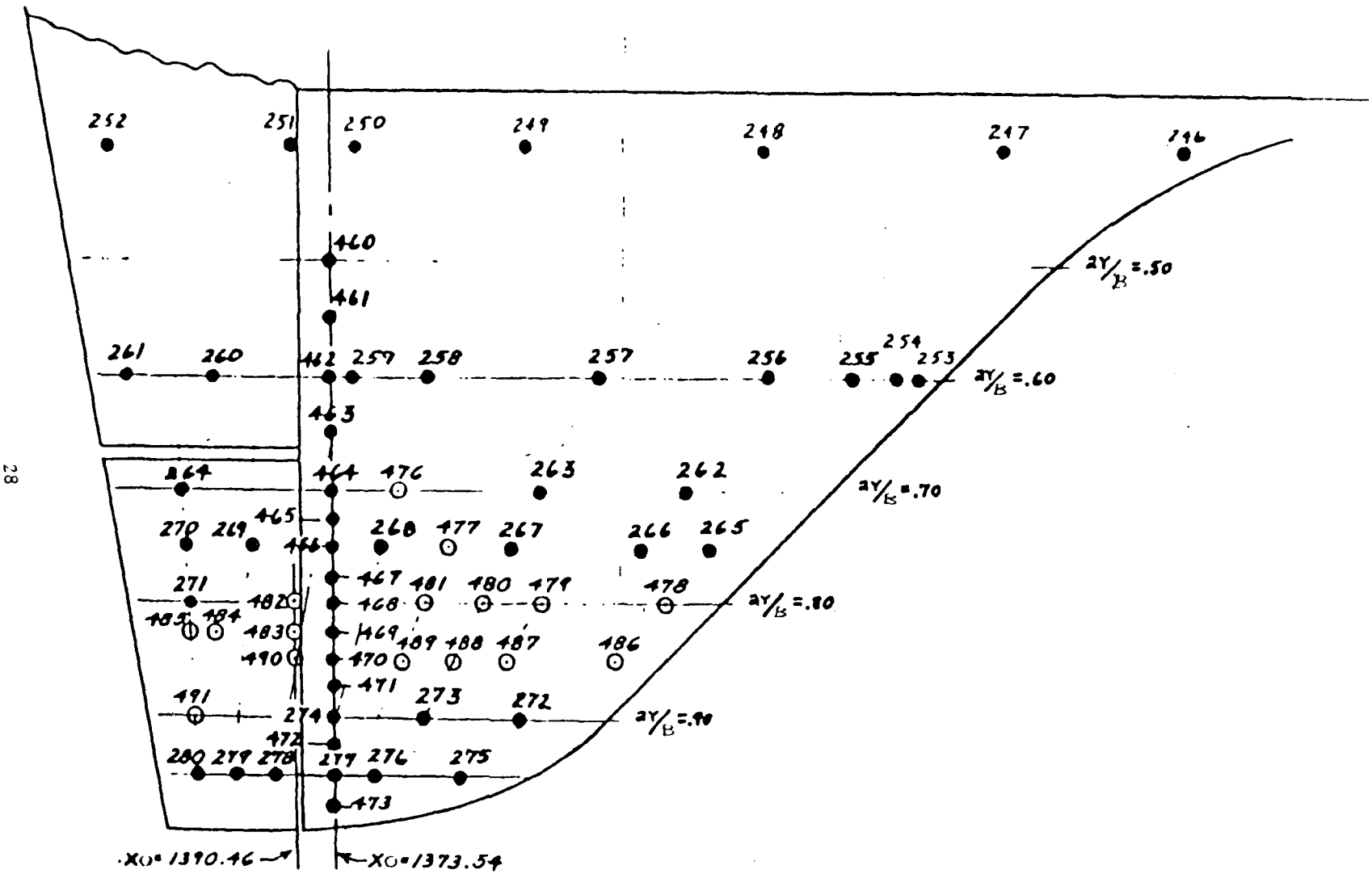

c. Upper Right Wing

Fig. 10. Continued

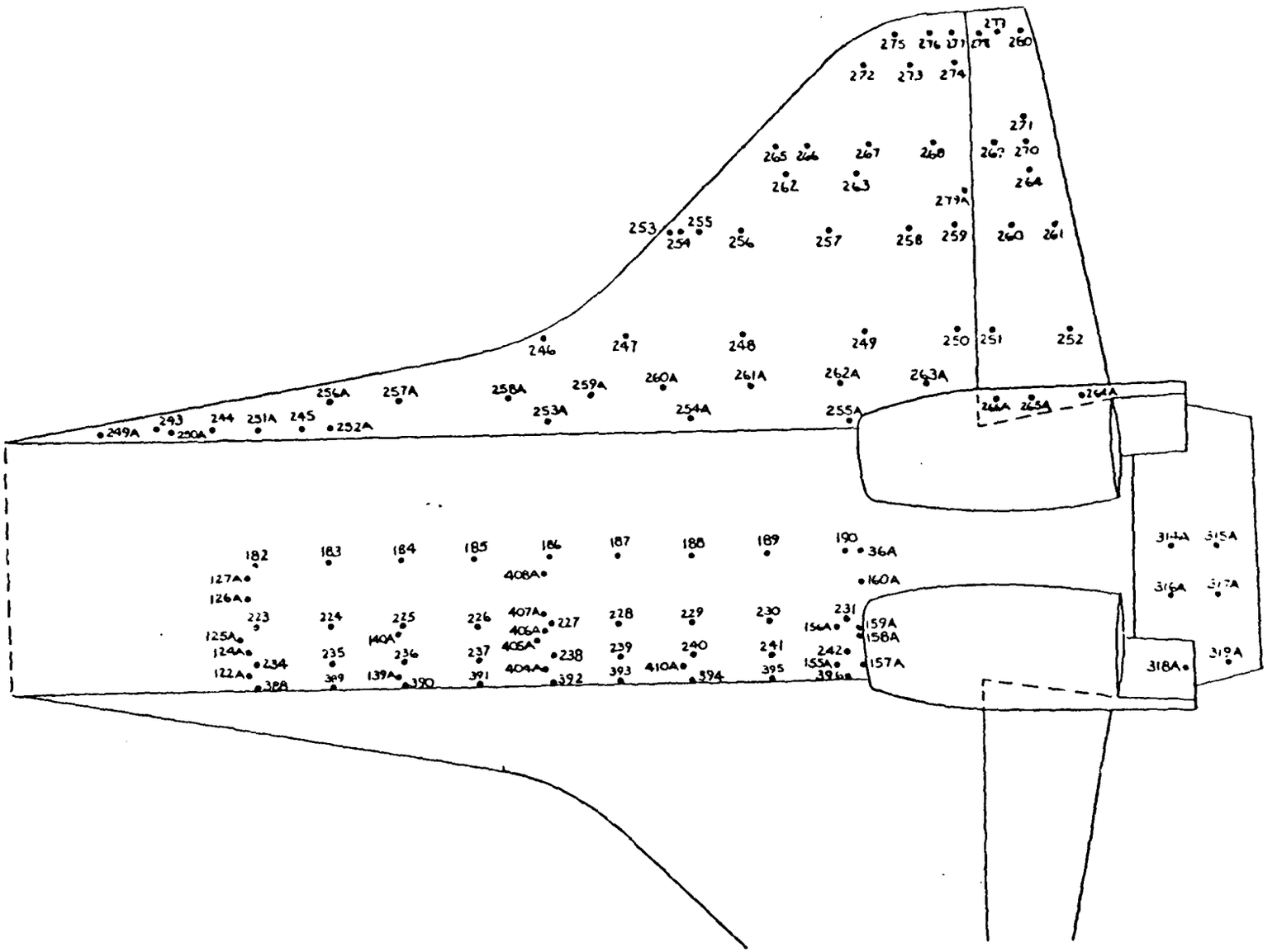

d. Upper Surface Thermocouples
Fig. 10. Continued

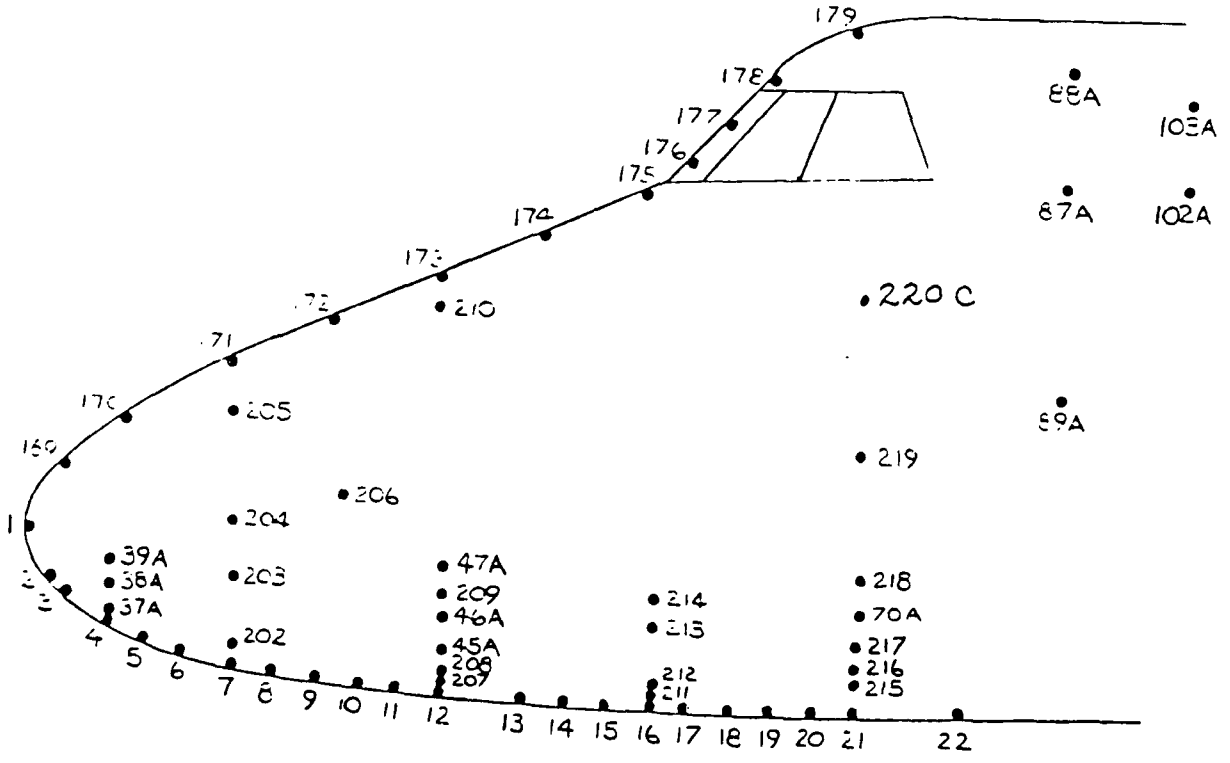

e. Forward Fuselage Side

Fig. 10. Concluded

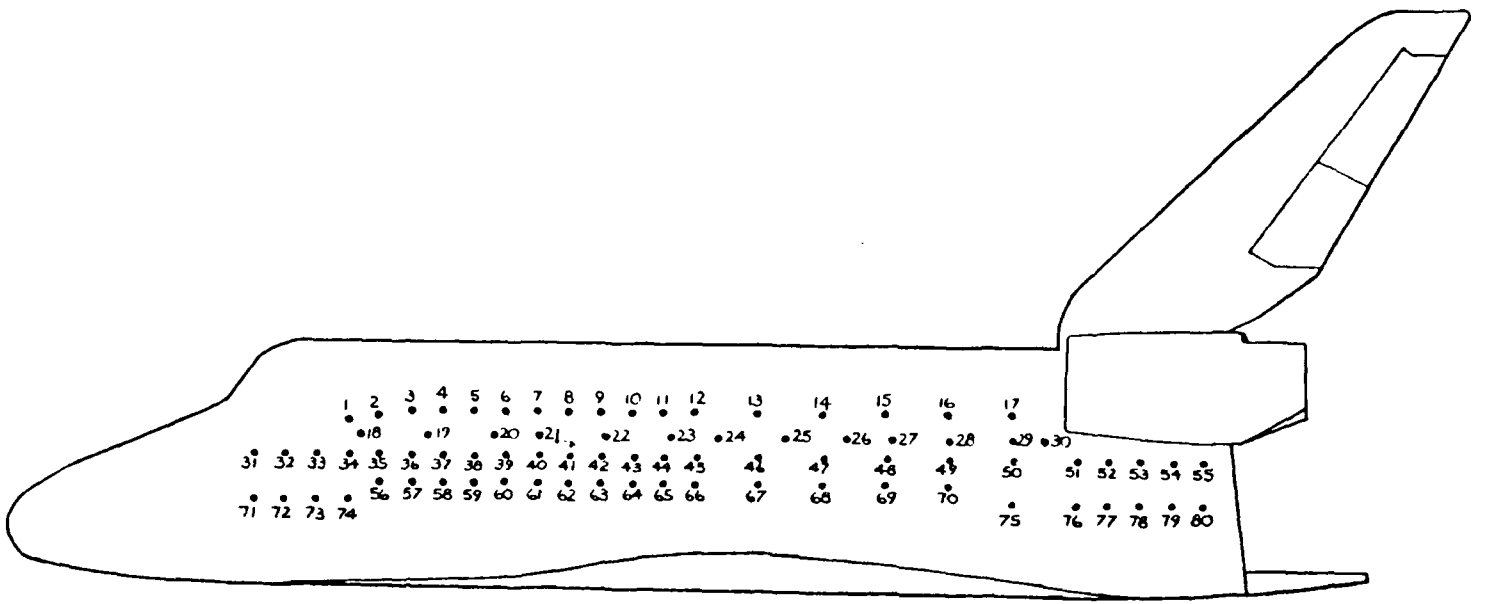

Fig. 11. Thermocouple Locations on 56-0 Model

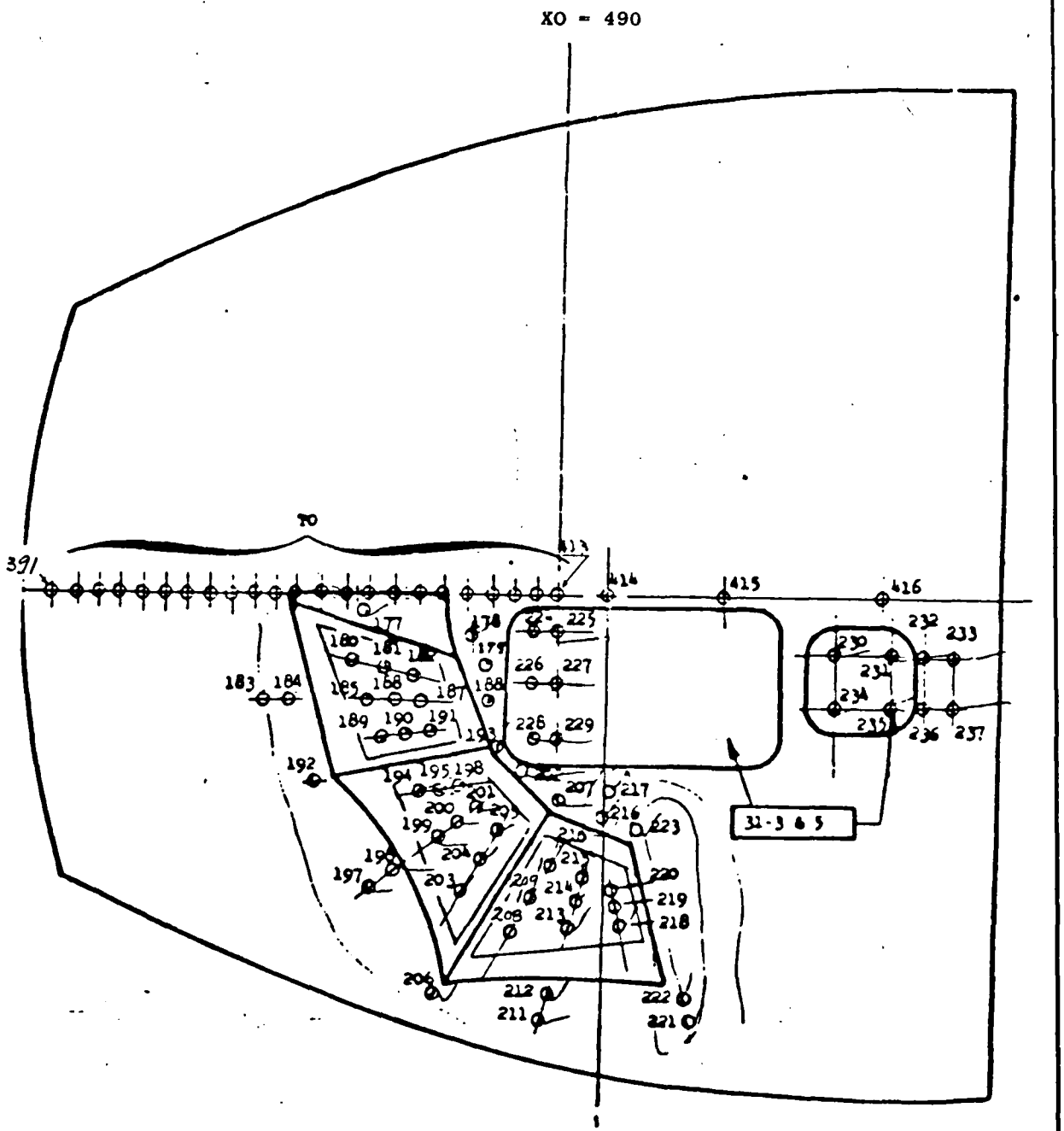

a. Canopy Thermocouple Locations

Fig. 12. Thermocouple Locations on 83-0 Model

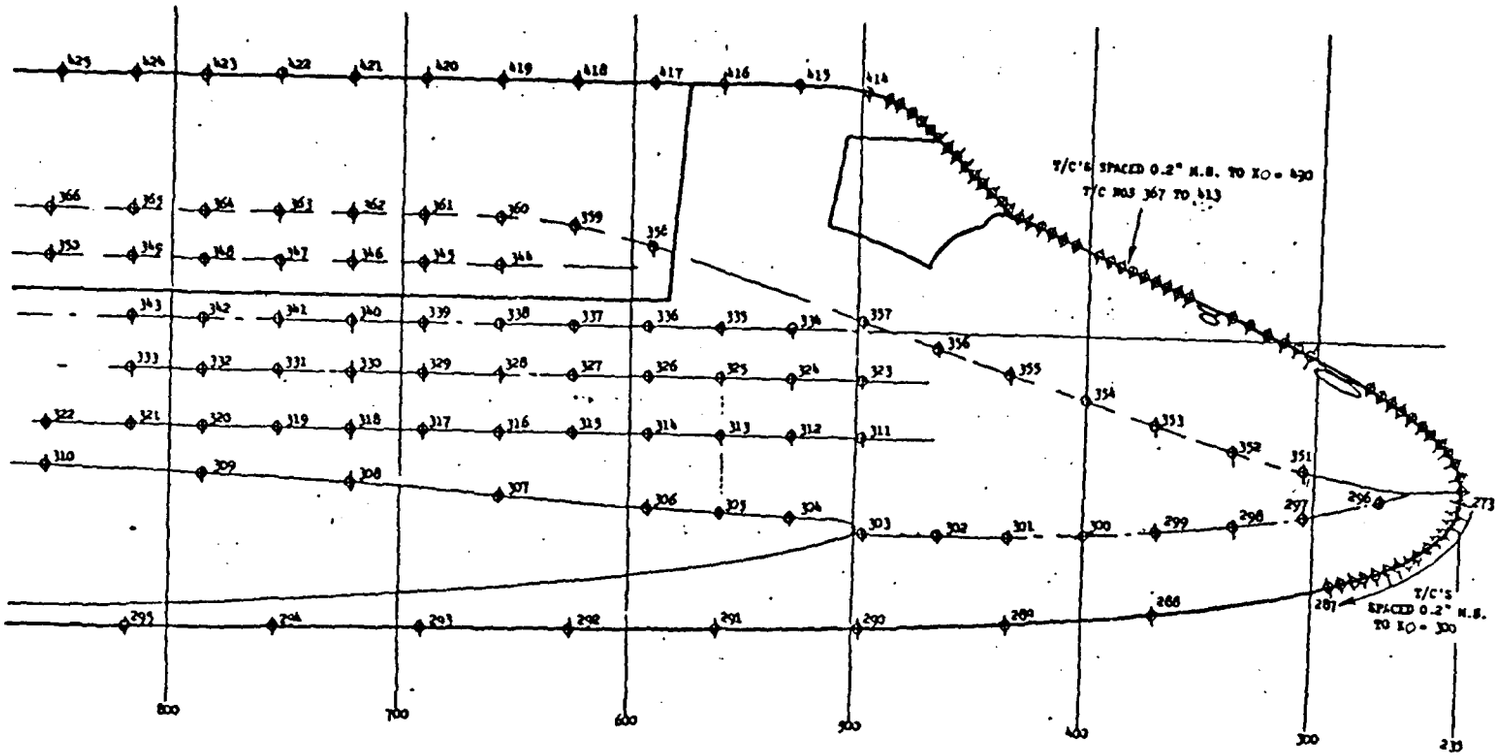

b. Thermocouple Locations on Fuselage Right Side

Fig. 12. Concluded

$$\text{Adjusted } H(TT) = \left[H(TT)_{\text{TAB DATA}} \right] \left[\frac{1}{\frac{H(TT)}{H(TRAX)}} \right]$$

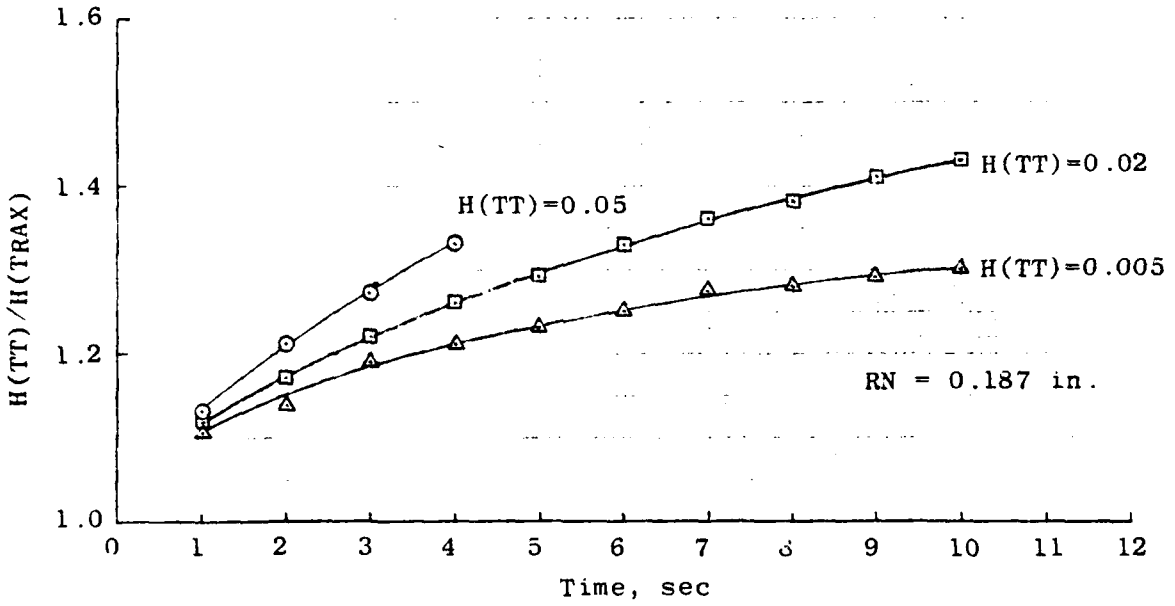

Fig. 13. Computed Influence of Semi-Infinite Slab Assumption on SILTS Pod Phase-Change Paint Data

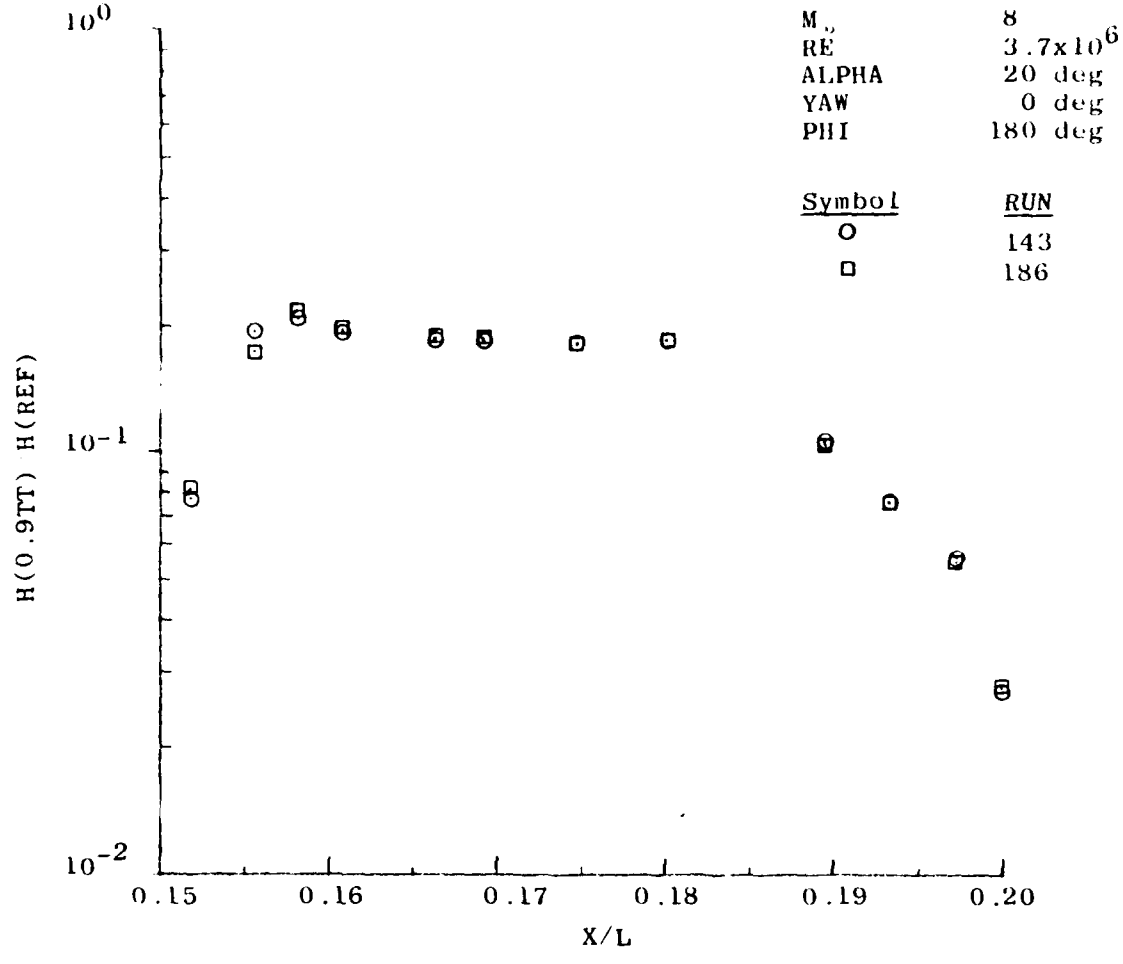

Fig.14. Data Repeatability on the 83-0 Model

APPENDIX II

TABLES

TABLE 1. ESTIMATED UNCERTAINTIES

a. Basic Measurements
Tunnel B

Parameter Designation	STEADY-STATE ESTIMATED MEASUREMENT*							Range	Type of Measuring Device	Type of Recording Device	Method of System Calibration
	Precision Index (S)			Bias (B)		Uncertainty ±(B + t_{95}S)					
	Percent of Reading	Unit of Measurement	Degree of Freedom	Percent of Reading	Unit of Measurement	Percent of Reading	Unit of Measurement				
ALPI, deg		0.025	>30				±0.05	±11	Potentiometer	Analog-to-digital converter into data acquisition system	Heidenhain rotary encoder ROD700 Resolution: 0.000 Overall accuracy: 0.001°
PHII, deg		0.15	>30				±0.3	±90			
Phase-change Paint Melt Temperature, °F	0+			±1.0		±1.0		All	Temperature Sensitive Paint		Supplied by paint manufacturer
$\sqrt{\rho CK}$, BTU/ft^2-sec$^{1/2}$-°R	0+			±10.0		±10.0					Supplied by Rockwell
PT, psia		0.02	>30		0.26		±0.3	0 < P ≤ 104	Bell & Howell variable capacitance pressure transducer	Analog to Digital Converter into Data Acquisition System	In-place application of multiple pressure levels measured with a pressure measuring device calibrated in the standards laboratory
		0.02	>30	0.25			±(0.25% + .08psi)	104<P<200			
		0.11	>30		0.58		±0.80	200<P≤232			
		0.11	>30	0.25			±(0.25% + 0.22psi)	232<P≤ 1000			
TI, °F		1	>30		2		±4	60-80	Chromel-Alumel Thermocouple	Doric Digital Thermometer	Thermocouple verification of NBS conformity/voltage substitution calibration
TIME, sec		$5x10^{-4}$	>30	[Runtime in sec] $(5x10^{-6})$		± [(Runtime in sec) $(5x10^{-6})+10^{-3}$] sec		milli-seconds to 365 days	System Donner time code reader	Digital Data Acquisition System	Instrument lab calibration against NBS
TT, °F		1	>30	0.375		±(0.375% + 2°F)		790-890	Chromel-Alumel Thermocouple	Digital Thermometer into Digital Data Acquisition System	Thermocouple verification of NBS conformity/voltage substitution calibration
Ts, °F		1	>30		2		±4	50-200	FE-CN Thermocouple	Low Level Multiplexer into Analog to Digital Converter into Data Acquisition System	
		1	>30		2		±4	50-200	CR-CN Thermocouple		

*Thompson, J. W. and Abernethy, R. B. et al. "Handbook Uncertainty in Gas Turbine Measurements." AEDC-TR-73-5 (AD 755356), February 1973.
Assumed to be zero

TABLE 1. Concluded

b. Calculated Parameters

Parameter Designation	STEADY-STATE ESTIMATED MEASUREMENT[a]							Range
	Precision Index (S)			Bias (B)		Uncertainty ±(B + t_{95}S)		
	Percent of Reading	Unit of Measurement	Degree of Freedom	Percent of Reading	Unit of Measurement	Percent of Reading	Unit of Measurement	
M		±0.020 ±0.010	>30		0[b] 0[b]		±0.04 ±0.02	7.83 8.0
RE, ft^{-1}	±0.70 ±0.36		>30	±0.56 ±0.45		±1.96 ±1.17		0.5×10^6 ft^{-1} 3.7×10^6 ft^{-1}
H(TT), H(.9TT), H(.85TT), BTU/ft^2-sec-^oR (Phase-Change Paint Technique)	±5.0		>30	±10.0		±20.0		All
H(TT), H(.9TT), H(.85TT), BTU/ft^2-sec-^oR (Thin-skin thermocouple technique)	±1.0		>30	±6.0		±8.0		$> 1 \times 10^{-3}$
	±4.0		>30	±6.0		±14.0		$1 \times 10^{-4} \rightarrow 1 \times 10^{-3}$
	±7.0		>30	±6.0		±20.0		$< 1 \times 10^{-4}$

[a] Abernethy, R. B. et al. and Thompson, J. W. "Handbook Uncertainty in Gas Turbine Measurements." AEDC-TR-73-5 (AD 755356), February 1973.

[b] Assumed to be zero

TABLE 2. 60-0 Model Thermocouple Locations

Vertical Tail			
T/C	X/C	Z/BV	b, in.
340	0.1	0.1	0.0315
341	0.3	0.1	0.0305
342	0.2	0.2	0.0302
345	0.4	0.2	0.0313
347	0.8	0.2	0.0315
349	0.2	0.3	0.0310
350	0.4	0.3	0.0310
351	0.5	0.3	0.0318
352	0.9	0.3	0.030
354	0.2	0.4	0.0315
356	0.5	0.4	0.0306
357	0.7	0.4	0.0290
358	0.9	0.4	0.0298
361	0.9	0.5	0.0315
363	0.1	0.6	0.0295
364	0.2	0.6	0.0303
365	0.4	0.6	0.0318
366	0.5	0.6	0.0315
367	0.7	0.6	0.0280
368	0.9	0.6	0.030
370	0.7	0.7	0.0275
371	0.9	0.7	0.0290
373	0.1	0.8	0.0293
374	0.4	0.8	0.0310
375	0.5	0.8	0.0325

Vertical Tail			
T/C	X/C	Z/BV	b, in.
376	0.7	0.8	0.0280
377	0.9	0.8	0.0290
378	0.1	0.9	0.0310
379	0.3	0.9	0.0305
380	0.5	0.9	0.0320
381	0.7	0.9	0.0308
382	0.9	0.9	0.0298
383	0.3	0.95	0.0313
384	0.5	0.95	0.0315
385	0.9	0.95	0.0330

OMS Pod				
T/C	XO, in.	YO, in.	ZO, in.	b, in.
1D	1312.5	103.47	437.62	0.039
2D	1312.5	105.65	451.57	0.025
3D	1313.4	99.92	463.35	0.041
4D	1314.2	90.04	474.41	0.043
5D	1315.4	81.42	485.17	0.028
6D	1316.2	69.87	492.67	0.027
7D	1317.8	56.21	497.18	0.027
8D	1319.2	42.82	495.93	0.031
9D	1322.7	113.14	434.29	0.023
10D	1322.9	113.90	446.10	0.033
11D	1323.2	115.62	459.73	0.029
12D	1323.4	110.38	472.01	0.036
13D	1324.9	101.55	482.44	0.031
14D	1326.3	92.10	492.89	0.024
15D	1327.3	80.93	501.43	0.026
16D	1328.5	68.91	508.10	0.029
17D	1331.3	54.30	510.38	0.029
18D	1332.4	41.74	504.13	0.028
19D	1336.5	114.14	437.45	0.027
20D	1336.1	120.76	449.66	0.034
21D	1336.0	124.01	462.41	0.026
22D	1335.5	119.09	475.11	0.028
23D	1336.8	110.33	485.84	0.030
24D	1337.4	99.43	495.69	0.029
25D	1338.4	83.08	504.61	0.031

OMS Pod				
T/C	XO, in.	YO, in	ZO, in.	b, in
26D	1339.9	76.58	512.79	0.030
27D	1341.3	64.69	517.49	0.026
28D	1343.2	50.13	514.51	0.030
29D	1344.6	38.66	506.42	0.029
30D	1348.9	111.69	427.05	0.015
31D	1348.0	119.71	438.95	0.023
32D	1346.9	126.40	451.59	0.029
33D	1346.9	128.97	461.66	0.027
34D	1347.9	123.26	478.95	0.029
35D	1348.6	114.89	488.55	0.031
36D	1350.0	104.37	498.45	0.031
37D	1350.9	93.15	507.16	0.032
38D	1351.9	81.63	515.29	0.031
39D	1353.3	68.97	521.14	0.029
40D	1355.5	55.02	520.43	0.033
41D	1356.8	42.64	512.69	0.028
42D	1360.9	115.72	428.93	0.016
43D	1360.7	124.34	441.15	0.023
44D	1359.7	130.58	452.74	0.032
45D	1359.5	133.66	466.33	0.033
46D	1359.8	128.57	479.54	0.031
47D	1360.0	119.66	489.71	0.023
48D	1361.1	109.53	499.35	0.026
49D	1362.4	98.70	508.42	0.027
50D	1363.8	86.07	516.66	0.029

TABLE 2. Continued

OMS Pod				
T/C	XO, in.	YO, in.	ZO, in.	b, in.
51D	1365.3	74.61	524.20	0.030
52D	1367.4	60.46	524.50	0.034
53D	1369.0	48.26	516.62	0.030
54D	1370.3	36.90	508.92	0.027
55D	1373.1	120.67	431.05	0.019
56D	1372.1	126.48	442.97	0.024
57D	1371.2	134.78	454.73	0.033
58D	1371.1	137.31	467.72	0.037
59D	1372.0	132.02	481.22	0.034
60D	1372.9	122.88	491.72	0.032
61D	1373.7	112.41	501.33	0.029
62D	1375.3	100.96	510.86	0.026
63D	1376.4	89.49	519.21	0.024
64D	1378.0	77.00	525.93	0.032
65D	1379.7	63.26	527.07	0.036
66D	1380.8	50.74	521.79	0.029
67D	1382.4	38.65	512.32	0.027
68D	1385.9	115.78	421.02	0.020
69D	1385.6	123.25	431.09	0.020
70D	1383.9	131.73	443.72	0.025
71D	1383.9	137.99	455.55	0.031
72D	1383.3	140.31	469.43	0.036
73D	1383.3	134.47	482.96	0.033
74D	1384.2	125.46	493.31	0.031
75D	1385.5	114.84	503.23	0.026

OMS Pod				
T/C	XO, in.	YO, in.	ZO, in	b, in.
76D	1386.9	104.23	511.85	0.025
77D	1396.2	140.63	456.75	0.034
78D	1395.7	142.72	471.17	0.040
79D	1395.4	137.55	483.60	0.035
80D	1407.8	143.07	458.22	0.035
81D	1408.2	144.85	472.53	0.040
82D	1408.3	138.82	486.10	0.035
83D	1420.6	145.46	460.62	0.035
84D	1420.3	146.41	474.10	0.040
85D	1420.7	140.53	487.50	0.034
86D	1433.1	147.19	461.84	0.034
87D	1432.7	147.95	474.38	0.038
88D	1433.3	142.34	488.33	0.031

Upper Wing			
T/C	X/C	2Y/B	b, in.
253	0.0250	0.6	0.009
254	0.050	0.6	0.0110
255	0.10	0.6	0.0210
256	0.20	0.6	0.0250
257	0.40	0.6	0.0270
258	0.60	0.6	0.0240
259	0.75	0.6	0.025
462	0.715	0.6	0.029
260	0.85	0.6	0.027
261	0.95	0.6	0.02
463	0.7	0.65	0.029
262	0.2	0.7	0.024
263	0.4	0.7	0.025
476	0.6	0.7	0.030
464	0.69	0.7	0.030
264	0.9	0.7	0.0280
465	0.68	0.725	0.029
265	0.10	0.75	0.023
266	0.20	0.75	0.023
267	0.40	0.75	0.025
477	0.5	0.75	0.028
268	0.60	0.75	0.022
466	0.67	0.75	0.027
269	0.8	0.75	0.024
270	0.9	0.75	0.028

Upper Wing			
T/C	X/C	2Y/B	b, in
467	0.66	0.775	0.024
478	0.1	0.8	0.031
479	0.3	0.8	0.032
480	0.4	0.8	0.032
481	0.5	0.8	0.032
468	0.65	0.8	0.021
482	0.725	0.8	0.025
469	0.64	0.825	0.021
483	0.715	0.825	0.026
484	0.85	0.825	0.025
485	0.90	0.825	0.029
486	0.1	0.85	0.032
487	0.2	0.85	0.030
488	0.4	0.85	0.030
489	0.5	0.85	0.030
470	0.63	0.85	0.025
490	0.7	0.85	0.023
471	0.62	0.875	0.026
272	0.2	0.9	0.025
273	0.4	0.9	0.025
274	0.6	0.9	0.03
472	0.575	0.925	0.027
275	0.2	0.95	0.023
276	0.4	0.95	0.03
277	0.95	0.95	0.025

TABLE 2 . Concluded

Upper Wing			
T/C	X/C	2Y/B	b, in.
278	0.7	0.95	0.028
279	0.8	0.95	0.029
280	0.9	0.95	0.028
473	0.45	0.975	0.020

Upper Fuselage			
T/C	X/L	PHI, deg	b, in.
183	0.45	180	0.026
185	0.55	180	0.026
186	0.60	180	0.025
187	0.65	180	0.024
188	0.70	180	0.025
189	0.75	180	0.0255
223	0.40	157.5	0.034
224	0.45	157.5	0.034
225	0.50	157.5	0.034
226	0.55	157.5	0.035
227	0.60	157.5	0.034
228	0.65	157.5	0.0325
230	0.75	157.5	0.03
231	0.80	157.5	0.032
234	0.40	135.0	0.03
235	0.45	135.0	0.03
236	0.50	135.0	0.036
237	0.55	135	0.035
238	0.6	135	0.031
240	0.7	135	0.03
241	0.75	135	0.32
242	0.8	135	0.32
389	0.45	114	0.033
390	0.50	114	0.036
391	0.55	114	0.0345

Upper Fuselage			
T/C	X/L	PHI, deg	b, in.
392	0.6	114	0.0335
393	0.65	114	0.0345
394	0.70	114	0.034
395	0.75	114	0.036
T/C	X/L	Y, in.	b, in.
124A	0.3974	1.128	0.0308
125A	0.3961	0.868	0.029
126A	0.3974	0.560	0.0285
139A	0.496	1.564	0.0337
140A	0.496	0.868	0.0291
404A	0.595	1.572	0.0301
405A	0.594	1.12	0.0322
406A	0.595	0.868	0.0285
407A	0.595	0.560	0.0284
408A	0.595	0.280	0.026
410A	0.695	1.572	0.0334
155A	0.79	1.572	0.0307
156A	0.79	0.808	0.0264
158A	0.819	1.218	0.0248
159A	0.819	0.868	0.0264
160A	0.819	0.308	0.0306
36A	0.817	0.0140	0.027d

Forward Fuselage Side			
T/C	X/L	ZO, in	b, in
210	0.1	410.0	0.037
220C	0.2	410.0	0.031
T/C	X/L	Y, in.	b, in.
89A	0.248	0.672	0.031
88A	0.247	1.101	0.026
102A	0.296	1.638	0.023
103A	0.296	0.467	0.015
T/C	X/L	Z, in.	b, in.
205	0.05	378.4	0.033
206	0.076	350.0	0.035

TABLE 3. 56-0 Model Thermocouple Locations

Fuselage Side			
T/C	X/L	ZO	b, in.
1	.275	437.5	.0215
2	.300	442.0	.0210
3	.325	445.0	.0217
4	.350	445.0	.0215
5	.375	445.0	.0212
6	.400	445.0	.0217
7	.425	445.0	.0215
8	.450	445.0	.0218
9	.475	445.0	.0219
10	.500	445.0	.0220
11	.525	445.0	.0220
12	.550	445.0	.0222
13	.600	445.0	.0220
14	.650	445.0	.0220
15	.700	445.0	.0228
16	.750	445.0	.0220
17	.800	445.0	.0230
18	.285	420.0	.0190
19	.337	420.0	.0189
20	.390	420.0	.0189
21	.426	420.0	.0190
22	.478	420.0	.020
23	.530	420.0	.020
24	.567	420.0	.0205
25	.620	420.0	.0205

Fuselage Side			
T/C	X/L	ZO	b, in.
26	.670	420.0	.0205
27	.705	420.0	.0207
28	.750	420.0	.0203
29	.800	420.0	.0202
30	.824	420.0	.0160
31	.200	400.0	.0210
32	.225	400.0	.0199
33	.250	400.0	.0199
34	.275	400.0	.0186
35	.300	400.0	.0180
36	.325	400.0	.0190
37	.350	400.0	.0192
38	.375	400.0	.0190
39	.400	400.0	.0189
40	.425	400.0	.0188
41	.450	400.0	.0195
42	.475	409.0	.0200
43	.500	400.0	.0200
44	.525	400.0	.0190
45	.550	400.0	.0200
46	.600	400.0	.0205
47	.650	400.0	.0210
48	.700	400.0	.0202
49	.750	400.0	.0205
50	.800	400.0	.0208

Fuselage Side			
T/C	X/L	ZO	b, in
51	.850	400.0	.0180
52	.875	400.0	.0180
53	.900	400.0	.0160
54	.925	400.0	.0170
55	.950	400.0	.0220
56	.300	372.5	.0170
57	.325	372.5	.0170
58	.350	372.5	.0170
59	.375	372.5	.0170
60	.400	372.5	.0170
61	.425	372.5	.0170
62	.450	372.5	.0172
63	.475	372.5	.0175
64	.500	372.5	.0180
65	.525	372.5	.0180
66	.550	372.5	.0190
67	.600	372.5	.0193
68	.650	372.5	.0190
69	.700	327.2	.0200
70	.750	372.5	.0200
71	.200	355	.0195
72	.225	355	.0190
73	.250	355	.0190
74	.275	355	.0180
75	.800	355	.0185

Fuselage Side			
T/C	X/L	ZO	b, in.
76	.850	355	.0188
77	.875	355	.0170
78	.900	355	.0172
79	.925	355	.0180
80	.950	355	.0190

TABLE 4. 83-0 Model Thermocouple Locations

Canopy			
T/C	RAY	LINE	b, in.
177	1	4	.0308
178	1	6	.0440
179	2	6	.0469
180	3	3	.0292
181	3	4	.0304
182	3	5	.0319
183	4	1	.0281
184	4	2	.0306
185	4	3	.0269
186	4	4	.0281
187	4	5	.0298
188	4	6	.0592
189	5	3	.0319
190	5	4	.0322
191	5	5	.0342
192	6	2	.0316
193	6	6	.0431
194	7	3	.0289
195	7	4	.0276
196	7	5	.0294
197	8	1	.0222
198	8	2	.0260
199	8	3	.0301
200	8	4	.0319
201	8	5	.0316

Canopy			
T/C	RAY	LINE	b, in.
202	8	6	.0283
203	9	3	.0278
204	9	4	.0348
205	9	5	.0349
206	10	2	.0297
207	10	6	.0300
208	11	3	.0301
209	11	4	.0308
210	11	5	.0299
212	12	2	.0302
213	12	3	.0297
211	12	1	.0279
216	12	6	.0318
217	12	7	.0319
218	13	3	.0309
219	13	4	.0315
220	13	5	.0308
222	14	2	.0276
223	14	6	.0304

Upper Centerline			
T/C	X/L	PHI	b, in
398	.1519	180	.0315
399	.1556	180	.0299
400	.1582	180	.0302
401	.1608	180	.0290
414	.2049	180	.0300
403	.1664	180	.0272
404	.1691	180	.0271
406	.1748	180	.0271
407	.1769	180	.0289
408	.1800	180	.0328
416	.250	180	.0262
411	.1894	180	.0336
412	.1931	180	.0312
413	.1972	180	.0300

Right Side			
T/C	X/L	ZO	b, in.
311	.20	355	.023
312	.225	355	.025
313	.250	355	.0296
314	.275	355	.0279
315	.300	355	.0308
319	.400	355	.0278
317	.350	355	.0311
318	.375	355	.0302
323	.200	378	.0259

Right Side			
T/C	X/L	ZO	b, in
324	.225	378	.0268
355	.150		.0273
326	.275	378	.0261
327	.300	378	.0266
328	.325	378	.0249
329	.350	378	.0306
330	.375	378	.0262
331	.400	378	.0269
357	.200		.0262
334	.225	400	.0255
335	.250	400	.0289
336	.275	400	.0262
337	.300	400	.0304
338	.325	400	.0269
339	.350	400	.0302
356	.175		.0311
341	.400	400	.0279
344	.325	425	.031
345	.350	425	.030
346	.375	425	.030
347	.400	425	.030
358	.275		.032
359	.300		.0310
360	325		.030
361	.350		.0305
362	.375		.030
364	.425		.032

TABLE 5. TEST DATA SUMMARY

a. Thin-Skin Thermocouple and Oil Flow Data Runs, 60-0 Model

ALPHA, DEG	DELTSB, DEG	REx10^{-6}, ft^{-1}	YAW, DEG						
			2	1	.5	0	-.5	-1	-2
20	49	3.7	14	12	10	1,2,17 105*,205*	4	6	8
25	49		15	13,16	11	3	5	7	9
20	0		94	48	42	18,54,100	24	30	36
25			95	49	43	19,104*, 206*	25	31	37
27.5			96	50	44	20,103*, 209*	26	32	38
30			97	51	45	21,102*, 200*,207*	27	33	39
32.5			98	52	46	22	28	34	40
35			99	53	47	23,101*, 201*,208	29	35	41
35		3.0	85,92,93	86	87		90	89	88
35		2.0	75	74	73	69,84	70	71	72
40		2.0	76	77	78	83,106*, 202*	82	81	79,80
40		1.0	55	56	57	61,62, 107*,203*	60	59	58
40		0.5			66	63,108*, 204*	64		

Delete: RUNS 65,67,68, and 91

* Oil Flow Data RUN

TABLE 5. Continued

b. Thin-Skin Thermocouple Data Runs, 83-0 Model

ALPHA, DEG	DELTSB, DEG	REx10^{-6}, ft^{-1}	YAW, DEG						
			2	1	.5	0	-.5	-1	-2
20	N.A.	3.7	180	178	167	143,186	154	155	166
25			181	177	168	144	153	156	179
27.5			182	176	169	145	152	157	
30			183	175	170	146,196*	151	158	163
32.5			164,184	159,174	171	147	150		162
35			165,185	173	172	148,197*	149	160	161
40						198*,199*			
35		3.0	187,194	188	189	193	192	191	190
20		2.0				124			
35		2.0	115	114	113	109,123	110	111	112
40		2.0	116	117	118	122	121	120	119
20		1.0				125			
40		1.0	132	131	130	126,133	127	128	129
20		.5				141			
40		.5	140	138	136	134,142	135	137	139

* Oil Flow DATA RUN
Delete: RUN 195

TABLE 5. Continued

c. Thin-Skin Thermocouple Data Runs, 56-0 Model

ALPHA, DEG	DELTSB, DEG	REx10^{-6}, ft^{-1}	YAW, DEG						
			2	1	.5	0	-.5	-1	-2
20	N.A.	3.7	246	245	234	210,252	221	222	233
25			247	244	235	211	220	223	232
27.5			248	243	236	212	219	224	231
30			249	242	237	213	218	225	230
32.5			250	241	238	214	217	226	229
35			251	240	239	215	216	227	228
35		3.0	253,260	254	255	259	258	257	256
35		2.0	267	266	265	261,275	262	263	264
40		2.0	268	269	270	274	273	272	271
40		1.0	282	281	280	276,283	277	278	279
40		.5	290	288	286	284,291	285	287	289

TABLE 5. Concluded

d. Phase Change Paint Data Runs

ALPHA, DEG	YAW, DEG	REx10^{-6}, ft^{-1}	PHASE CHANGE PAINT TEMPERATURE, ^{o}F						
			250	300	350	450	550	600	700
35	0	0.6		317					
35	-2	↓		318					
35	0	1.0			309				
35	-2				314				
40	0		311	313	310				
40	-2	↓		312					
30	0	2.0						305	
35	0						306		
40	0	↓				308	307		
30	0	3.0							300
30	-2								304
35	0							302	301
35	-2	↓						303	
30	0	3.7			292	293	294		295
30	-2								299
35	0								296,297
35	-2	↓							298

Delete: RUNS 315 and 316

TABLE 6

MODEL MATERIAL THERMOPYSICAL PROPERTIES

Novamide 700-55

TPC, °F	$\sqrt{PCK}$, Btu/ft^2-sec$^{1/2}$-°R
250	0.057
300	0.058
350	0.059
450	0.060
550	0.060
600	0.059
700	0.058

APPENDIX III

REFERENCE HEAT-TRANSFER COEFFICIENTS

In presenting heat-transfer coefficient results it is convenient to use reference coefficients to normalize the data. Equilibrium stagnation point values derived from the work of Fay and Riddell* were used to normalize the data obtained in this test. These reference coefficients are given by:

$$H(REF) = \frac{0.17173(PT2)^{1/2}(MUTT)^{0.4}\left[1 - \frac{P}{PT2}\right]^{0.25}\left[0.2235 + (1.35 \times 10^{5})(TT+560)\right]}{(RN)^{1/2}(TT)^{0.15}}$$

and

$$STFR = \frac{H(REF)}{(RHO)(V)\ [0.2235 + (1.35 \times 10^{-5})(TT + 560)]}$$

where

PT2	Stagnation pressure downstream of a normal shock wave, psia
MUTT	Air viscosity based on TT, lb_f-sec/ft^2
P	Free-stream pressure, psia
TT	Tunnel stilling chamber temperature, °R
RN	Reference nose radius, (0.0175 ft or 0.04 ft determined by model scale)
RHO	Free-stream density, lbm/ft^3
V	Free-stream velocity, ft/sec

*Fay, J. A. and Riddell, F. R. "Theory of Stagnation Point Heat Transfer in Dissociated Air," Journal of the Aeronautical Sciences, Vol. 25, No. 2, February 1958.

APPENDIX IV

SAMPLE TABULATED DATA

ARO, INC. - AEDC DIVISION
A SVERDRUP CORPORATION COMPANY
VON KARMAN GAS DYNAMICS FACILITY
ARNOLD AIR FORCE STATION, TENNESSEE
NASA/RI OH109 HEATING
PAGE 1

DATE COMPUTED 10-DEC-80
TIME COMPUTED 08:49:50
DATE RECORDED 28-OCT-80
TIME RECORDED 4:38:52
PROJECT NUMBER V41B-69

RUN	MODEL	MACH NO	PT,PSIA	TT,DEGR	ALPPB	ALPI	PHII	ALPHA	YAW
100	60-0	7.97	828.1	1357.7	30.00	9.94	0.09	20.06	0.01

T	P	Q	V	RHO	MU	RE	H(REF)	STFR
DEGR	PSIA	PSIA	FT/SEC	LBM/FT3	LB-SEC/FT2	FT-1	(RN= 0.0175FT)	(RN= 0.0175FT)
99.00	0.087	3.858	3889.	2.364E-03	7.967E-08	3.586E+06	4.880E-02	2.129E-02

DELTAE	DELTBF	DELTASB
0.0	0.0	0.0

TC NO	TW DEG R	DTW/DT DEG S	QDOT BTU/ FT2-S	H(TT) BTU/FT2-S-DEG R	H(TT) /H(REF)	H(.9TT) BTU/FT2-S-DEG R	H(.9TT) /H(REF)	H(.85TT) BTU-FT2-S-DEG R	H(.85TT) /H(REF)	VERTICAL TAIL X/C	VERTICAL TAIL Z/BV	SKIN THICK NESS
340	503.1	12.722	1.762	2.062E-03	0.0422	2.451E-03	0.0502	2.707E-03	0.0555	0.1000	0.1000	0.0315
341	500.0	5.973	0.800	9.323E-04	0.0191	1.108E-03	0.0227	1.223E-03	0.0251	0.3000	0.1000	0.0305
344	498.9	7.081	0.938	1.092E-03	0.0224	1.297E-03	0.0266	1.432E-03	0.0293	0.2000	0.2000	0.0302
345	496.8	3.688	0.506	5.875E-04	0.0120	6.975E-04	0.0143	7.695E-04	0.0158	0.4000	0.2000	0.0313
347	496.1	1.237	0.171	1.981E-04	0.0041	2.351E-04	0.0048	2.594E-04	0.0053	0.8000	0.2000	0.0315
349	500.7	6.112	0.832	9.707E-04	0.0199	1.153E-03	0.0236	1.273E-03	0.0261	0.2000	0.3000	0.0310
350	498.5	3.339	0.454	5.284E-04	0.0108	6.276E-04	0.0129	6.926E-04	0.0142	0.4000	0.3000	0.0310
351	497.7	2.357	0.329	3.820E-04	0.0078	4.536E-04	0.0093	5.005E-04	0.0103	0.5000	0.3000	0.0318
352	498.0	1.669	0.220	2.554E-04	0.0052	3.033E-04	0.0062	3.346E-04	0.0069	0.9000	0.3000	0.0300
354	503.9	7.041	0.975	1.142E-03	0.0234	1.358E-03	0.0278	1.500E-03	0.0307	0.2000	0.4000	0.0315
356	504.5	2.335	0.316	3.702E-04	0.0076	4.401E-04	0.0090	4.860E-04	0.0100	0.5000	0.4000	0.0308
357	505.5	1.184	0.151	1.773E-04	0.0036	2.109E-04	0.0043	2.330E-04	0.0048	0.7000	0.4000	0.0290
358	501.8	1.790	0.234	2.739E-04	0.0056	3.254E-04	0.0067	3.593E-04	0.0073	0.9000	0.4000	0.0298
361	506.7	1.682	0.233	2.743E-04	0.0056	3.263E-04	0.0067	3.606E-04	0.0074	0.9000	0.5000	0.0315
363	533.2	26.193	3.449	4.184E-03	0.0857	5.009E-03	0.1026	5.556E-03	0.1139	0.1000	0.6000	0.0295
364	518.9	13.073	1.756	2.093E-03	0.0429	2.497E-03	0.0512	2.764E-03	0.0566	0.2000	0.6000	0.0303
365	517.6	7.904	1.113	1.325E-03	0.0272	1.580E-03	0.0324	1.749E-03	0.0358	0.4000	0.6000	0.0318
366	518.9	6.128	0.855	1.020E-03	0.0209	1.217E-03	0.0249	1.347E-03	0.0276	0.5000	0.6000	0.0315
367	514.4	2.362	0.292	3.466E-04	0.0071	4.134E-04	0.0085	4.573E-04	0.0094	0.7000	0.6000	0.0280
368	510.6	1.983	0.262	3.099E-04	0.0063	3.690E-04	0.0076	4.079E-04	0.0084	0.9000	0.6000	0.0300
370	518.8	3.867	0.471	5.618E-04	0.0115	6.703E-04	0.0137	7.419E-04	0.0152	0.7000	0.7000	0.0275
373	536.1	21.787	2.854	3.474E-03	0.0712	4.162E-03	0.0853	4.619E-03	0.0946	0.1000	0.8000	0.0293
374	525.2	8.593	1.184	1.423E-03	0.0292	1.700E-03	0.0348	1.883E-03	0.0386	0.4000	0.8000	0.0310
375	522.7	6.395	0.923	1.105E-03	0.0226	1.320E-03	0.0270	1.462E-03	0.0300	0.5000	0.8000	0.0325
376	519.6	4.032	0.580	5.972E-04	0.0122	7.126E-04	0.0146	7.899E-04	0.0162	0.7000	0.8000	0.0280
377	517.1	3.417	0.439	5.220E-04	0.0107	6.225E-04	0.0128	6.898E-04	0.0141	0.9000	0.8000	0.0290
378	541.2	23.769	3.303	4.045E-03	0.0829	4.852E-03	0.0994	5.389E-03	0.1104	0.1000	0.9000	0.0310
379	523.1	7.888	1.069	1.280E-03	0.0262	1.529E-03	0.0313	1.693E-03	0.0347	0.3000	0.9000	0.0305
380	510.7	1.831	0.259	3.052E-04	0.0063	3.635E-04	0.0074	4.01FE-04	0.0082	0.5000	0.9000	0.0320
381	518.7	2.912	0.397	4.73HE-04	0.0097	5.652E-04	0.0116	6.256E-04	0.0128	0.7000	0.9000	0.0308
382	518.1	3.141	0.415	4.938E-04	0.0101	5.891E-04	0.0121	6.520E-04	0.0134	0.9000	0.9000	0.0298
383	523.8	8.016	1.115	1.337E-03	0.0274	1.597E-03	0.0327	1.769E-03	0.0362	0.3000	0.9500	0.0313

1. Thin-Skin Thermocouple Data

ARO, INC. - AEDC DIVISION
A SVERDRUP CORPORATION COMPANY
VON KARMAN GAS DYNAMICS FACILITY
ARNOLD AIR FORCE STATION, TENNESSEE
NASA/RI OH-10S HEATING TEST
PAGE 1

DATE COMPUTED 24-NOV-80
TIME COMPUTED 04:43:34
DATE RECORDED 24-NOV-80
TIME RECORDED 2:50: 3
PROJECT NUMBER V41B-G9

RUN	MODEL	MACH NO	PI,PSIA	TT,DEGR	ALPHA	ALPI	PHII	ALPHA	YAW
292	56-0	7.97	429.2	1363.7	30.00	0.00	-0.02	30.00	0.00

T (DEG R)	P (PSIA)	Q (PSIA)	V (FT/SEC)	RHO (LBM/FT3)	MU (LB-SEC/FT2)	RE (FT-1)	H(REF) (RN=0.0175FT)	STEP (RN=0.0175FT)	(PCK)1/2 (BTU/FT2-SEC**.5-R)
99.58	0.0868	3.863	3960.	2.3535-03	8.013E-08	3.569E+06	4.489E-02	2.135E-02	0.0470

- - - - - PHASE CHANGE PAINT DATA - - - - -

CAMERA	RUN NO	PAINT TEMP (DEGF)	INITIAL TEMP (DEGF)	THAR(TT)	BETA(TT)	THAR(.90TT)	BETA(.90TT)	THAR(.85TT)	BETA(.85TT)
TOP	292	350.	72.	3.333E-01	4.070E-01	3.986E-01	5.285E-01	4.419E-01	6.220E-01
OS	290	350.	72.	3.333E-01	4.070E-01	3.986E-01	5.285E-01	4.419E-01	6.220E-01
NOS	291	350.	72.	3.333E-01	4.070E-01	3.986E-01	5.285E-01	4.419E-01	6.220E-01

PIC NO	TIME	TIMEEXP	S(TT)	H(TT)/HREF	H(.90TT)	H(.90TT)/HREF	H(.85TT)	H(.85TT)/HREF
OS 1(350)	1.77		MODEL HAS NOT REACHED CENTERLINE					
TOP 1(350)	1.77		MODEL HAS NOT REACHED CENTERLINE					
NOS 1(350)	1.76		MODEL HAS NOT REACHED CENTERLINE					
TOP 2(350)	2.35		MODEL HAS NOT REACHED CENTERLINE					
OS 2(350)	2.35		MODEL HAS NOT REACHED CENTERLINE					
NOS 2(350)	2.36		MODEL HAS NOT REACHED CENTERLINE					
TOP 3(350)	2.93		MODEL HAS NOT REACHED CENTERLINE					
OS 3(350)	2.93		MODEL HAS NOT REACHED CENTERLINE					
NOS 3(350)	2.94		MODEL HAS NOT REACHED CENTERLINE					
INJECT TIME = 3.19								
TOP 4(350)	3.51	1.72	1.490E-02	0.2986	1.895E-02	0.3877	2.231E-02	0.4563
OS 4(350)	3.51	1.72	1.490E-02	0.2986	1.895E-02	0.3877	2.231E-02	0.4563
NOS 4(350)	3.52	1.73	1.454E-02	0.2974	1.888E-02	0.3861	2.221E-02	0.4545
TOP 5(350)	4.09	2.30	1.242E-02	0.2582	1.639E-02	0.3353	1.929E-02	0.3946
OS 5(350)	4.09	2.30	1.242E-02	0.2582	1.639E-02	0.3353	1.929E-02	0.3946
NOS 5(350)	4.10	2.31	1.258E-02	0.2573	1.633E-02	0.3341	1.922E-02	0.3932
OS 6(350)	4.67	2.87	1.124E-02	0.2409	1.465E-02	0.2997	1.724E-02	0.3527
TOP 6(350)	4.67	2.88	1.124E-02	0.2307	1.464E-02	0.2996	1.724E-02	0.3526
NOS 6(350)	4.68	2.89	1.125E-02	0.2301	1.461E-02	0.2988	1.719E-02	0.3517
OS 7(350)	5.25	3.46	1.029E-02	0.2105	1.336E-02	0.2733	1.573E-02	0.3217
TOP 7(350)	5.25	3.46	1.029E-02	0.2104	1.336E-02	0.2733	1.572E-02	0.3216
NOS 7(350)	5.26	3.47	1.027E-02	0.2100	1.333E-02	0.2727	1.569E-02	0.3210
TOP 8(350)	5.83	4.04	9.522E-03	0.1946	1.236E-02	0.2529	1.455E-02	0.2977
OS 8(350)	5.83	4.04	9.522E-03	0.1948	1.236E-02	0.2529	1.455E-02	0.2977
NOS 8(350)	5.84	4.05	9.502E-03	0.1944	1.234E-02	0.2524	1.452E-02	0.2971
TOP 9(350)	6.41	4.62	8.903E-03	0.1821	1.156E-02	0.2365	1.361E-02	0.2783
OS 9(350)	6.41	4.62	8.903E-03	0.1821	1.156E-02	0.2365	1.361E-02	0.2783
NOS 9(350)	6.42	4.63	8.893E-03	0.1818	1.154E-02	0.2361	1.359E-02	0.2778
OS 10(350)	6.99	5.20	8.392E-03	0.1717	1.090E-02	0.2229	1.282E-02	0.2624
TOP 10(350)	6.99	5.20	8.389E-03	0.1716	1.089E-02	0.2229	1.282E-02	0.2623
NOS 10(350)	7.00	5.21	8.378E-03	0.1714	1.088E-02	0.2226	1.280E-02	0.2619

2. Phase Change Paint Data


DATE
ILME
8